Order Number 9207142

The mechanism of *ermC* mRNA degradation in *Bacillus subtilis*

Zen, Kuo Huei, Ph.D.

City University of New York, 1991

U·M·I

300 N. Zeeb Rd.
Ann Arbor, MI 48106

The Mechanism of *ermC* mRNA Degradation in *Bacillus subtilis*

by

Kuo Huei Zen

A dissertation submitted to the Graduate Faculty in Biomedical Sciences in partial fulfillment of the requirements for the degree of Doctor of Philosophy, The City University of New York.

1991

This manuscript has been read and accepted for the Graduate Faculty in Biomedical Sciences in satisfaction of the dissertation requirement for the degree of Doctor of Philosophy.

AUGUST 13, 1991
Date

Chair of Examining Committee

August 13 1991
Date

Executive Officer

George Acs

James Bieker

Terry Krulwich

Supervisory Committee

The City University of New York

ABSTRACT

The Mechanism of *ermC* mRNA Degradation in *Bacillus subtilis*

by

Kuo Huei Zen

Advisor: Professor David H. Bechhofer

The *ermC* gene encodes an rRNA methyltransferase and confers erythromycin resistance on the host by reducing the affinity of ribosome for erythromycin. A previous study had shown that *ermC* mRNA is stabilized in the presence of erythromycin, an inducer of *ermC* gene expression. The induced stability of *ermC* mRNA requires a ribosome stalled in the *ermC* leader peptide sequence. Our working hypothesis was that the 5' end of *ermC* mRNA is the target of decay and ribosome stalling in the leader peptide sequence protects *ermC* mRNA from ribonucleolytic decay in the 5'-to-3' direction.

In order to test this hypothesis, several insertion mutations of the *ermC* leader region were constructed and used to examine how ribosome stalling affects *ermC* mRNA stability. Using constructs in which the ribosome stall site was internal rather than at the 5' end of the message, it was shown that ribosome stalling provides stability to sequences downstream but not upstream of the ribosome stall site. In a construct that contained a ribosome stall site at the 5' end, in addition to an internal ribosome stall site, the full-length RNA was

stabilized in the presence of erythromycin. These results strongly suggest that *ermC* mRNA is degraded either by a 5'-to-3' exoribonuclease or by an endoribonuclease that binds to 5' end and make endoribonucleolytic cleavages as it progresses in the 5'-to-3' direction, and that a stalled ribosome at the 5' end protects against this type of decay.

To provide biochemical evidence for this conclusion, *B. subtilis* extracts were prepared, and RNase substrates were synthesized that could be used to identify a 5' end-requiring RNase activity in *B. subtilis* extracts. First, it was shown that *ermC* mRNA synthesized by in vitro transcription is degraded in *B. subtilis* extracts. Second, an RNA-DNA joint molecule was synthesized that contained an RNA moiety in its 5' region and a ssDNA moiety in its 3' region. This joint molecule is degraded to a ssDNA molecule under the condition that degradation of DNA was inhibited, indicating that the RNA moiety of the joint molecule is degraded either by a 5'-to-3' exoribonuclease or by an endoribonuclease activity in *B. subtilis* extracts. To distinguish between these two possibilities, a circular RNA molecule was constructed. This circular RNA was not degraded in *B. subtilis* extracts although the linear RNA containing the same sequence as the circular RNA was degraded. Taken together, these results suggest the existence of a 5'-to-3' exoribonuclease in *B. subtilis*.

ACKOWLEDGEMENTS

I am deeply gratefully to Dr. David Bechhofer, who has directed my thesis cheerfully and generously. I have warm memories of stimulating discussions with him during the entire time I have worked in the laboratory.

I am also grateful to Drs. George Acs, James Bieker and Terry Krulwich for serving on my graduate student committee and for sharing their suggestions and time with me. I am also indebted to the Department of Biochemistry that provided all the equipment for my thesis research. The discussion during the departmental seminar also gave me helpful suggestions during this work.

I am especially grateful to Dr. Krulwich, who provided me the opportunity to study at the Mount Sinai School of Medicine. The completion of my study is due in large part to her encouragement and support.

It is a pleasure to express my sincere appreciation to my colleagues, Kim Hue and John DiMari. I have benefitted greatly from the advice, assistance, criticism, and encouragement of my colleagues.

Special thanks go to my parents for their years of care and encouragement. Finally, I must acknowledge with deep appreciation the encouragement, understanding, patience and good spirit of my wife and my children, who have truly shared in the completion of this thesis.

TABLE OF CONTENTS

LIST OF FIGURES

PAGE

ABBREVIATIONS

AKD buffer	10 mM Tris OAc (pH 8.0), 15 mM $Mg(OAc)_2$, 60 mM KOAc, 1 mM dithiothreitol, and 0.20 mM phenylmethylsulfonyl fluoride
ATP	adenosine triphosphate
bp	base-pair
Bs-RNase III	RNase III-like ribonuclease in *B. subtilis*
B. subtilis	*Bacillus subtilis*
CAT	chloramphenicol acetyltransferase
Cm	chloramphenicol
CTP	cytosine triphosphate
dA	deoxyadenine
dATP	deoxyadenosine triphosphate
dCTP	deoxycytosine triphosphate
dGTP	deoxyguanosine triphosphate
DNA	Deoxyribonucleic acid
ds	double-stranded
dT	deoxythymine
dTTP	deoxythymidine triphosphate
E. coli	*Escherichia coli*
EDTA	ethylenediamine tetraacetate
Em	erythromycin
GMP	guanosine monophosphate
GTP	guanosine triphosphate
Km	kanamycin
methylase	23 rRNA methyltransferase
MLS	macrolide-lincosamide-streptogramin B
mRNA	messenger ribonucleic acid
nt	nucleotide
OAc	acetate
PIPES	piperazine-N-N'-bis(2-ethane sulfonic acid)
PNPase	polynucleotide phosphorylase
RF	replicative form
RNA	ribonucleic acid
RNase	ribonuclease
SD	Shine-Dalgarno sequence
SD1	Shine-Dalgarno sequence for *ermC* leader peptide
SD2	Shine-Dalgarno sequence for *ermC* methylase

ss	single-stranded
TE	10 mM Tris-HCl (pH 7.5) and 1 mM EDTA
Tris	tris(hydroxymethyl)aminomethane
U	unit
UTP	uridine triphosphate

CHAPTER ONE
INTRODUCTION

1-1 Messenger RNA decay in procaryotes

Messenger RNA stability plays an important role in the posttranscriptional regulation of both procaryotic and eucaryotic gene expression (for review, see King et al., 1986; Brawerman, 1987; Belasco and Higgins, 1988; Brawerman, 1989; Cleveland and Yen, 1989; Saini et al., 1990). In the absence of translational regulation, the rate of synthesis of a protein depends on the concentration of the mRNA that encodes it, which is determined by a balance between the rates of mRNA synthesis and degradation. Although a number of elegant studies during the past two decades have been directed towards elucidating the mechanism of mRNA decay, very little is known about the cellular factors involved in mRNA breakdown and the structural determinants of mRNA (in)stability.

For most bacterial mRNAs, the half-lives are very short, in the range of 2 to 3 minutes. The high turnover rate of bacterial mRNA ensures a rapid adaptation to the environmental change. However, in *Escherichia coli*, the message stability can differ by as much as a factor of 50 (Nilsson et al, 1984).

mRNA decay in *E. coli* is hypothesized to proceed through the concerted action of endo- and exoribonucleases. Despite the identification of a number of ribonucleases in *E. coli* (Deutscher, 1985, 1988), only four have been shown to play a role in mRNA decay: RNase II (Donovan and Kushner, 1983), polynucleotide phosphorylase (Kinscherf and Apirion, 1975; Donovan and Kushner,

1986), RNase III (Dunn and Studier, 1973; Portier et al., 1987; Bardwell et al., 1989; Regnier and Grunberg-Manago, 1989) and RNase E (Mudd et al., 1988; Regnier and Hajnsdorf, 1991). Polynucleotide phosphorylase and RNase II are exoribonucleases that degrade mRNA in the 3'-to-5' direction, whereas RNase III and RNase E are endoribonucleases.

From the studies with *E. coli* mutants, polynucleotide phosphorylase and RNase II are now thought to be involved in the breakdown of mRNA to the mononucleotide level. Cells lacking only one of these enzymes are viable, whereas the absence of both enzymes leads to loss of viability and the accumulation of mRNA fragments (Kinscherf and Apirion, 1975; Donovan and Kushner, 1986). It has been shown that the chemical half-lives of specific mRNAs are increased in *E. coli* strains carrying mutations in the genes that encode polynucleotide phosphorylase and RNase II (Arraiano et al., 1988). Both polynucleotide phosphorylase and RNase II are processive exoribonucleases initiating breakdown at the 3' end of an RNA molecule, and both are influenced by secondary structure in the RNA. However, the enzymes are different in that RNase II hydrolyses RNA to nucleoside monophosphates, whereas polynucleotide phosphorylase ultilizes a phosphorolytic mechanism releasing nucleoside diphosphates.

The structural feature of mRNA responsible for resistance to attack by 3'-to-5' exoribonucleases is now relatively well understood. A stem-loop structure such as a rho-independent terminator at the 3' end of many messages or repetitive extragenic palindromes can function as a barrier against 3'-to-5' exoribonucleolytic digestion and

the molecules lacking such a structure are extremely vulnerable to exonucleolytic attack (Chen et al., 1988; Newbury et al., 1987; Mott et al, 1985; Wong and Chang, 1986). The stem-loop structure also appears to impart stability to selected regions of polycistronic mRNAs. In the case of the *malEFG* operon of *E. coli* (Newbury et al., 1987) and the *puf* operon of *Rhodobacter capsulatus* (Belasco et al., 1985; Chen et al., 1988; Chen and Belasco, 1990; Klug and Cohen, 1990; Klug and Cohen, 1991), the 5'-region of a polycistronic mRNA is more stable than the 3'-region. An intercistronic structure, which is located at the 3'-boundary of the stable segment of these transcripts, causes the stabilization of upstream RNA, presumably by providing a barrier against the action of 3'-to-5' exoribonucleases. Thus the difference in mRNA stability can contribute to differential gene expression within a polycistronic operon. For *papBA* mRNA of *E. coli* (Baga et al., 1988), the 5'-segment of the transcript is preferentially degraded presumably by an endoribonucleolytic cleavage followed by 3'-to-5' exoribonucleolytic degradation to ensure lower expression of the *papB* gene.

On the other hand, secondary structures in some RNAs are the targets recognized by several endoribonucleases. RNase III and RNase E are two endoribonucleases that have been implicated in the endoribonucleolytic processing of mRNA. In some mRNAs, a cleavage by RNase III in regions that can fold into secondary structures is the limiting step of decay (Portier et al, 1987; Bardwell et al., 1989; Regnier and Grunberg-Manago, 1989; Schmeissner et al., 1984). RNase E also cleaves mRNA in the vicinity of secondary structures (Mudd et al., 1988; Regnier and Hajnsdorf, 1991) and many

transcipts of phage T4 are functionally and chemically stabilized in an RNase E deficient strain (Mudd et al., 1990). Although RNase III and RNase E are involved in the decay of some mRNAs, the major role of these two endoribonucleases is thought to be the processing of ribosomal RNA precursors (King et al., 1986).

The product of the gene designated *ams* (*a*ltered *m*essage *s*tability) has also been shown to be involved in mRNA decay in *E. coli* (Kuwano et al., 1977; Ono and Kuwano, 1979; Arraiano et al., 1988). Strains carrying the temperature-sensitive *ams* mutation have a longer chemical half-life at the nonpermissive temperature (Kuwano et al., 1977). Therefore, Kushner and coworkers suggested that the Ams protein was either an RNase or a positive regulator of other RNases (Arraiano et al., 1988). Recent genetic studies have shown that the Ams protein and RNase E turn out to be encoded by the same structural gene of *E. coli* (Babitzke and Kushner, 1991; Taraseviciene et al., 1991; Melefors and von Gabain, 1991).

As mentioned before, the decay of some mRNAs in *E. coli* is initiated by endoribonucleolytic cleavage at specific sites. Since no 5'-to-3' exoribonucleases have yet been identified in *E. coli* (Deutscher, 1985; Belasco and Higgins, 1988), it is believed that mRNA decay is accomplished by 3'-to-5' exoribonucleases either at the 3' end of the message or at 3' ends generated by endoribonucleolytic cleavages.

The idea that mRNA decay in *E. coli* proceeds in a net 5'-to-3' direction evolved from studies on the polycistronic *trp* operon which showed that the 5' end could be attacked before the synthesis of the 3' end was completed (Morikawa and Imamoto, 1969; Morse et al., 1969). Using a similar approach, the same conclusion has been

reached in studies on polycistronic *lac* mRNA (Kennell, 1986). Based on the study of *lac* mRNA decay in *E. coli*, Kennell and coworkers proposed a model that any region of mRNA which is free of ribosomes is vulnerable to degradation (Cannistraro et al., 1986; Subbarao and Kennell, 1988), In this model, ribosomes physically protect mRNA from ribonuclease attack. When ribosome loading is interrupted by endonucleolytic cleavage at the ribosome binding site, the newly unprotected 5' ends of mRNA are "chopped off" by endonucleolytic cleavage as the ribosomes move down the message. Although mRNA stability has been attributed in some cases to occupancy by ribosomes, untranslated regions are not necessarily more labile than translated regions (Nilsson et al., 1987; Lundberg et al., 1988).

Despite the large amount of work in recent years devoted to understanding the mechanism of mRNA breakdown in *E. coli*, relatively little attention has been given to the study of mRNA deacy in *B. subtilis*, a Gram positive bacteria. Studies on *B. subtilis* polycistronic *sdh* mRNA decay suggested that the 5'-segment of the *sdh* mRNA might be more susceptible to ribonuclease attack than the 3'-segment and serves as an important determinant for the stability of the whole message (Melin et al., 1990). Loading of ribosomes on the 5' region has been shown to be sufficient to afford stability to the whole mRNA, suggesting that ribosomes protect the 5' region from initiation of decay. Based on the studies on *ermA* and *ermC* mRNA decay in *B. subtilis* (see Section 1-2), the ribosome stalled at the 5' leader peptide sequences protects mRNAs from attack by an RNase which recognizes the 5' end of the message (Bechhofer and Zen, 1989;

Sandler and Weisblum, 1989). On the other hand, from studies on *cry* mRNA decay in *B. subtilis*, Wong and Chang (1986) proposed that the stem-loop structure of the 3' end of *cry* mRNA provides protection against exonucleolytic degradation from the 3' end.

As mentioned previously, polynucleotide phosphorylase and RNase II are two 3'-to-5' exoribonucleases that are involved in mRNA decay in *E. coli.* Deutscher and Reuven (1991) demonstrated recently that RNase II activity represents close to 90% of the total exoribonuclease activity and polynucleotide phosphorylase only accounts for about 10% of the total activity of *E. coli* extract. The *B. subtilis* equivalent of polynucleotide phosphorylase exists in cell extracts. However, the *B. subtilis* equivalent of RNaseII is not present in cell extracts. It is not known whether a *B. subtilis* equivalent of polynucleotide phosphorylase plays a role in mRNA decay. The only endoribonuclease which has been characterized from *B. subtilis* is an RNase III-like ribonuclease (Bs-RNase III) which was shown to be involved in cleavage of several phage SP82 early mRNAs (Panganiban and Whiteley, 1983a and b). Studies on *pur* operon mRNA decay intermediates in *B. subtilis* also suggested that an unknown endoribonuclease might be involved in *pur* operon mRNA degradation (Ebbole and Zalkin, 1988). Like mRNA decay in *E. coli*, it seems that mRNA degradation in *B. subtilis* can proceed by a number of mechanisms.

1-2 The control of *ermC* mRNA stability in *B. subtilis*

The *ermC* gene, which is carried on plasmid pBD142 in *B. subtilis* (Fig. 1), was chosen as a model to study the mechanism of

Figure 1. Physical map of pBD142.

Arrows show direction and extent of resistance genes for erythromycin (*ermC*) and chloramphenicol (CAT). Origin of replication (*ori*) and the relevant restriction sites are shown. pBD144 is a low-copy version of pBD142.

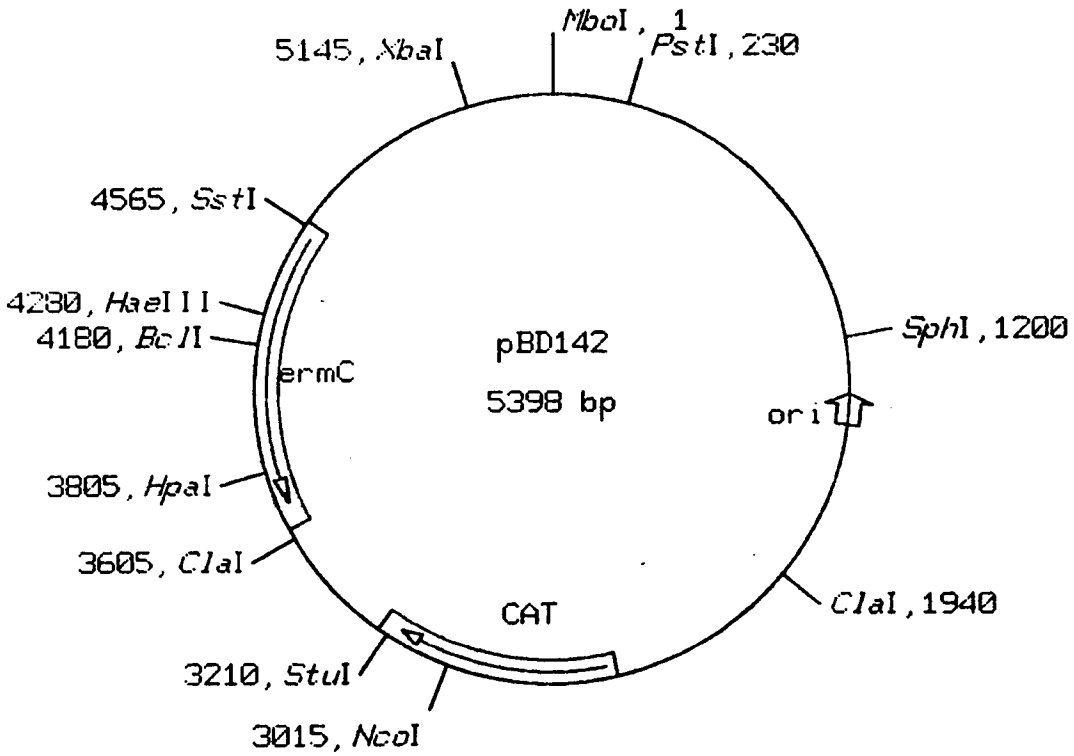
MboI , 1
PstI , 230
SphI , 1200
ClaI , 1940
NcoI
3015
StuI
3210
CAT
ClaI
3605
HpaI
3805
ermC
BclI
4180
HaeIII
4280
SstI
4565
XbaI
5145
pBD142
5398 bp
ori

mRNA decay and the factors involved in mRNA stability in this organism. The *ermC* gene encodes an rRNA methyltransferase (methylase) (Shivakumar and Dubnau, 1981) which catalyzes the N^6,N^6-dimethylation of a specific adenine residue in 23S ribosomal RNA and confers macrolide-lincosamide-streptogramin B (MLS) resistance on the host by reducing the affinity of ribosomes for these antibiotics (Weisblum et al., 1971; Shivakumar et al., 1980). Synthesis of methylase is inducible by the addition of subinhibitory concentrations of erythromycin (Em), an MLS antibiotic.

Expression of the *ermC* gene product is regulated at the post-transcriptional level (for review, see Bechhofer, 1990). To explain the induction of methylase translation, a "translational attenuation" mechanism has been proposed (Weisblum, 1983; Dubnau, 1984). The *ermC* mRNA has a 141-nucleotide (nt) leader sequence (Fig. 2A) which is located between the promoter and AUG start codon for the methylase. This leader sequence contains a Shine-Dalgarno sequence (SD1), a short reading frame which codes for a 19-amino-acid peptide and a second Shine-Dalgarno sequence (SD2) just 5' to the methylase start codon. In the absence of Em, the *ermC* mRNA leader sequence is folded in a stable stem-loop structure which makes SD2 unavailable for translation (Fig. 2B). In the presence of Em, an Em-bound ribosome stalls in the leader sequence, thereby opening the stem-loop structure to allow ribosome binding at SD2 and translation of the methylase coding sequence. Induction by Em results in a 20-fold increase in methylase translation.

The induction of methylase translation is accompanied by an increase in *ermC* mRNA stability (Shivakumar et al., 1980; Bechhofer

Figure 2. Translational attenuation model.

(A) Uninduced structure of *ermC* mRNA regulatory region (Dubnau, 1984). Ribosome-binding sites for the leader peptide coding sequence (SD1) and the methylase coding sequence (SD2) are indicated. Initiation and stop codons are underlined. (B) *ermC* gene regulation. Em (Δ) binds to unmethylated ribosomes, causing ribosome stalling in the leader peptide sequence. The resulting conformational change of the leader mRNA frees SD2 for translation. The possibility of a second ribosome binding at SD1 and stalling behind the Em-bound ribosome is depicted (Bechhofer and Zen, 1989). Methylated (•) ribosomes cannot be bound by Em and are not involved in induction.

A

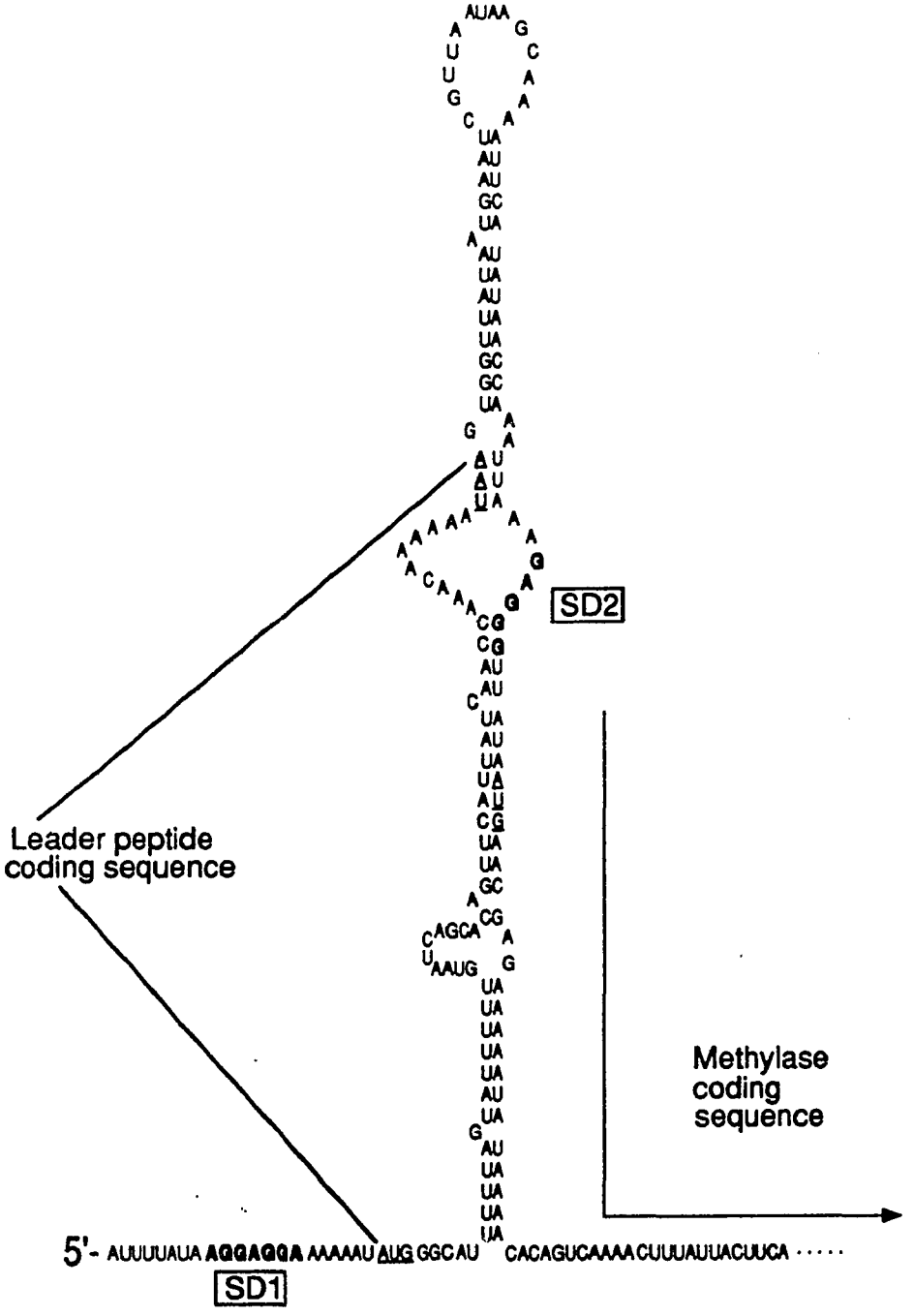
Leader peptide coding sequence
SD2
Methylase coding sequence
5'- AUUUUAUA AGGAGGA AAAAAU AUG GGC AU CACAGUCAAAA CUUUAUUACUUCA .....
SD1

B

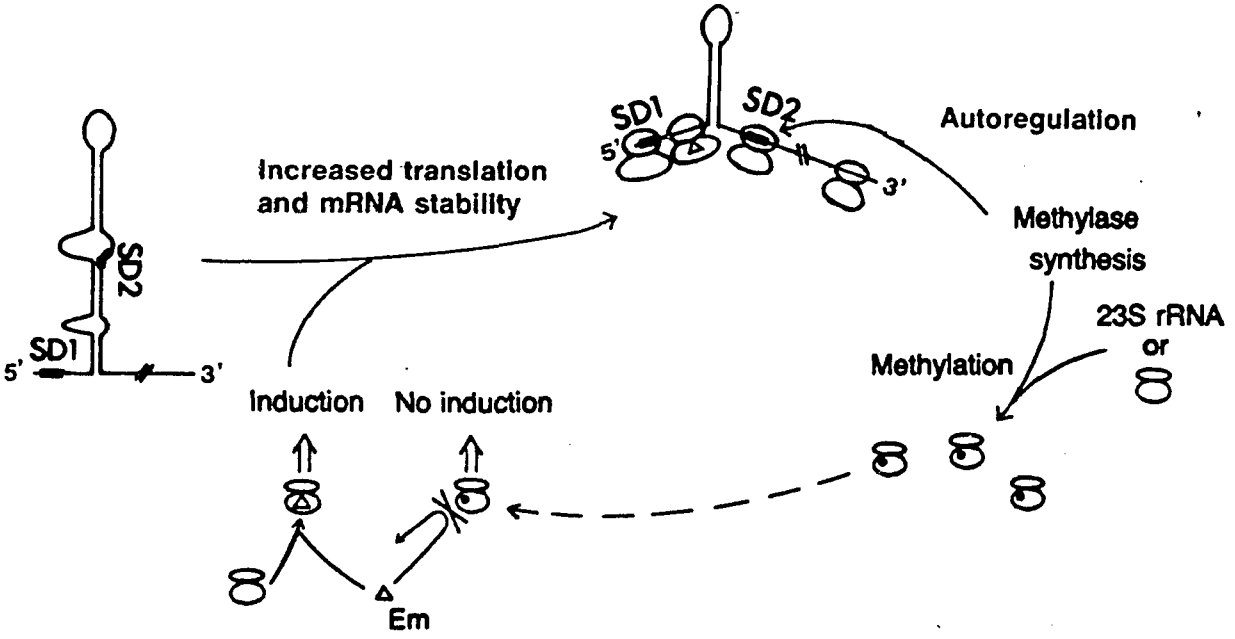
SD2
SD1
5'
3'
Increased translation
and mRNA stability
SD1
SD2
5'
3'
Autoregulation
Methylase
synthesis
23S rRNA
or
Methylation
Induction
No induction
Em

and Dubnau, 1987). Upon the induction by Em, the half-life of *ermC* mRNA is increased from 2 min to 40 min. Induced stabililization of *ermC* mRNA occurs in the absence of methylase translation but requires translation of the leader peptide and ribosome stalling in the leader sequence. In a strain carrying a translational fusion between the 5' end (360 nucleotides) of *ermC* and the *E. coli lacZ* coding sequence, several RNAs that have a 5' *ermC* sequence and different 3' sequences are also stabilized in the presence of Em, indicating that the 5' end of *ermC* mRNA is sufficient to confer *cis*-dominant stabilization. Similar results have been published for *ermA*, another Em resistance gene (Sandler and Weisblum, 1988).

The finding that ribosome stalling in the leader sequence is required for stabilization of *ermC* mRNA can be explained in several ways (Bechhofer and Dubnau, 1987). One of the models is that the presence of a stalled ribosome physically protects the mRNA from an endoribonuclease which recognizes the specific sequence or the secondary structure of the leader sequence. This possibility has been ruled out recently by the analysis of various mutations in the *ermC* leader region (Hue and Bechhofer, 1991). Analysis of deletion mutants showed that ribosome stalling causes induction of *ermC* mRNA stability in the absence of *ermC* leader RNA secondary structure. The *ermC* mRNA is also inducibly stable in a strain in which the Em stall site is located entirely upstream of the stem-loop sequence, indicating that the leader stem-loop sequence is not the target of endoribonucleolytic attack. Alternatively, the 5' end of the message could be the target for initiation of processive decay in the 5'-to-3' direction. A stalled ribosome in the leader peptide sequence

could cause a backup of another ribosome loading at SD1 such that the 5' end of *ermC* mRNA, which is only 9 nucleotides upstream of SD1, is protected. Although "two-ribosome stalling" model is depicted in Figure 2B, it is not clear yet whether one or two ribosomes stall in the leader sequence (see discussion in Section 4-1). It has been shown in vitro that Em-induced ribosome stalling in the leader region results in RNase protection of the 5' end of the message (Narayanan and Dubnau, 1987).

From the studies on *ermC* mRNA stability of some insertion mutations in the *ermC* leader region, it has been suggested that the decay of *ermC* mRNA in *B. subtilis* occurs either by a 5'-to-3' exoribonuclease or by an endoribonuclease that tracks in the 5'-to-3' direction from the 5' end, and that a stalled ribosome at the 5' end protects against this type of decay (Bechhofer and Zen, 1989). Induced mRNA stability of a related MLS resistance gene, *ermA*, occurs by a similar mechanism (Sandler and Weisblum, 1989). Some 5'-to-3' exoribonucleases have been characterized in eucaryotes (Lasater and Eichler, 1984; Stevens and Maupin, 1987; Murthy et al., 1991), Although no 5'-to-3' exoribonucleases have been identified in *E. coli*, it is possible that a 5'-to-3' exoribonuclease exists and plays a role in mRNA decay in *B. subtilis*, a Gram positive bacteria. Biochemical identification of a 5'-to-3' exoribonuclease activity in *B. subtilis* extracts is necessary to confirm this conclusion.

CHAPTER TWO
MATERIALS AND METHODS

2-1 Bacterial strains

The *B. subtilis* host for plasmids pSD100, pSD125, pSD132, and pSD192 was IS75, which is *hisA1 leu metB5*. Strain BE8 was a transformant of BD170, which is *trpC2 thr-5*. The minicell-producing host was CU403, which is *thyA thyB metB5 divIVBI* (Reeve et al., 1973). The *E coli* strain for making uridine-containing DNA was CJ236, which is F-*dut ung1 thi-1 relA1/pCJ105* (Cm^r) (Raleigh et al., 1989). The strain for phage M13 propagation was JM109, which is F' *traD36 lac^{q}Δ(lacZ)M15 proAB/ recA1 endA1 gyrA96* (Nal^r) *thi hsdR17* (rk-mk+) *supE44 relA1 Δ(lac-proAB)* (Yanish-Perron et al., 1985).

2-2 Standard procedures

The preparation of *B. subtilis* growth media and competent *B. subtilis* culture was as described (Dubnau and Davidoff-Abelson, 1971). Solid medium was tryptose blood agar base (TBAB, Difco). Concentrations of Em, chloramphenicol (Cm), and Kanamycin (Km) used for selection were 5 μg/ml. Plasmid DNA was isolated and purified from stationary cultures grown at 32°C using the sodium dodecyl sulfate-NaCl method (Guerry et al., 1973) followed by CsCl-ethidium bromide density gradient centrifugation as described (Gryczan et al., 1978). Transformation of *B. subtilis* by plasmids was as described (Contente and Dubnau, 1979). The preparation and storage of minicells, [^{3}H]leucine incorporation into minicell proteins

and sodium dodecyl sulfate-polyacrylamide gel analysis of these products were exactly as described (Shivakumar et al., 1979).

Oligonucleotides that were used for directed nucleotides changes were purchased from the DNA Core Facility of the Brookdale Center for Molecular Biology, Mount Sinai School of Medicine. Oligonucleotide-directed mutagenesis was performed as described (Kunkel et al., 1987). After mutagenesis, M13 replicative form (RF) containing the mutagenized DNA was prepared and the fragments were isolated and used to replace the corresponding fragments in plasmids that were transformed back into *B. subtilis*.

2-3 Plasmids

The plasmids used in this thesis are summarized in Appendix A (Chapter 5). Plasmid pSD100 is a derivative of plasmid pBD142 (Bechhofer and Zen, 1989). Plasmid pBD142 (see Fig. 1) consists of pE194 *cop*-6 (Gryczan et al., 1982) plus the chloramphenicol resistance gene of pC194 on a *Cla*I fragment. A synthetic 30-base-pair fragment, prepared by B. Goldschmidt of the Department of Biochemistry, New York University Medical School, consisted of the following sequence:

-10 *Pvu*II

5'-CGTGCTATAATTATACTAATCAGCTGAGCT-3'

3'-TCGAGCACGATATTAATATGATTAGTCGAC-5'

This fragment, which has overlapping *Sac*I ends, was cloned into the pBD142 *Sac*I site which is located between the *ermC* -10 and -35 promoter sequences. The -10 sequence in the inserted fragment was the proper distance from the upstream -35 sequence, and the

original *ermC* -10 sequence was still present downstream of the inserted fragment. The pBD142 derivative that contained the inserted 30-bp fragment was plasmid pSD1. By reverse transcriptase analysis, it was found that *ermC* mRNA encoded by pSD1 has two transcriptional start sites 30 nucleotides apart. Apparently, the original *ermC* -10 sequence, although it does not have a proper -35 sequence upstream of it, can promote transcription of *ermC* in this construct. To avoid the problem of two *ermC* RNAs, the original *ermC* -10 sequence was inactivated by using oligonucleotide-directed mutagenesis (Kunkel et al., 1987) to change the -10 region sequence (TATAATTATA) to an *Eco*RI site (GAATTC). The pSD1 derivative that contained this *Eco*RI site was pSD78.

The unique *Pvu*II site present on the inserted 30-bp fragment was used to clone isolated *Alu*I fragments of pC194. One clone chosen for further study (plasmid pSD100) contained a tandem insert of a 275-bp *Alu*I sequence, which consists of nucleotides 2711 to 2437 of the published pC194 sequence (Horinouchi and Weisblum, 1982b). Although the published sequence does not have an *Alu*I site at nucleotide 2711, restriction endonuclease mapping of pC194 revealed that there was a *Pvu*II site (which is also an *Alu*I site) at that position. The C-G base pair at position 2711 in the published sequence must therefore be incorrect. The orientation of the inserted *Alu*I fragment was determined by the asymmetric *Taq*I site (see Fig. 3). Upon *Mbo*I digestion of some preparations of pSD100 and pSD132 DNAs, an additional minor band was observed that represented a small deletion of the inserted pC194 DNA. This probably arose because the insert is a tandem repeat. An internal deletion of this

sort could explain the intermediate-sized RNAs detected in the blot analyses of pSD100- and pSD132-encoded *ermC* mRNAs (see Fig. 4 and 6).

The BAL-31-deleted plasmid used for the experiment for which the results are shown in Fig. 4C was made by digesting pSD100 with *Pvu*II, treating it briefly with BAL-31, and religating. Plasmid molecules that had small deletions were isolated, and one of these, pSD125, was chosen for further study. An *Mbo*I fragment from pSD125 (*Mbo*I-*Bcl*I in Fig. 3), which contained the upstream sequence of pSD100 (minus a 25-bp deletion) and the first 360 nucleotides of *ermC*, was cloned into the *Bam*HI site of M13mp18 for sequencing.

To construct plasmid pSD132 (see Fig. 6), I used plasmid pBD452, which was kindly provided by F. Breidt of the Public Health Research Institute of New York. Plasmid pBD452 is a derivative of pBD142 that has a *Sal*I linker inserted 6 nucleotides downstream from the end of the *ermC* leader peptide coding sequence. A *Sal*I-*Hae*III digest of pBD452 yielded three fragments, the smallest of which represented the 5' end of the methylase coding sequence. The two larger *Sal*I-*Hae*III fragments of pBD452 were purified from an agarose gel and ligated with a *Sal*I-*Hae*III fragment from an M13mp18 RF derivative that contained the pSD125 fragment (see above). A plasmid, pSD132, was recovered that had the promoter and the 5' end of *ermC* up to the *Sal*I site of pBD452, followed by the upstream sequence of pSD125, followed by the wild-type *ermC* leader region and the methylase coding sequence. The sequence between the 5'-proximal and the internal ribosome stalling site in

pSD132 was identical to the upstream sequence of pSD100, except for the 25-bp deletion present in pSD125.

Figure 7A summarizes the scheme employed to construct plasmid pSD192. First, the sequence (ACTAATT) between *ermC* -10 and SD1 was changed to *Bgl*II and *Hin*dIII sites (AGATCTAAGCTT) by oligonucleotide-directed mutagenesis. The pBD452 derivative that contained the *Bgl*II and *Hin*dIII sites was pSD155. A *Pst*I-*Sal*I digest of pSD155 yielded two fragments and an *Eco*RI-*Pst*I digest of pSD78 also yielded two fragments. The smaller *Pst*I-*Sal*I fragment of pSD155 and the larger *Eco*RI-*Pst*I fragment of pSD78 were purified from an agarose gel and ligated together with a 470-bp *Sal*I-*Eco*RI fragment from an M13mp19 RF derivative, which contained an *Xba*I-*Eco*RI fragment of pUB110. A plasmid, pSD172, was recovered that has the promoter and 5' leader sequence of *ermC* up to the *Sal*I site of pSD155, followed by an insert from pUB110, followed by the *ermC* leader sequence and the methylase coding sequence. A *Bgl*II-*Hin*dIII digest of pSD172 was ligated with a 340-bp *Bam*HI-*Hin*dIII fragment from an M13mp19 RF derivative that contains the *Bam*HI-*Xba*I fragment of pUB110. The pSD172 derivative that contained an insert from pUB110 between *ermC* -10 and the first SD1 was pSD192.

Plasmid pYH3 is a derivative of plasmid pIBI31 (see Fig. 9). Plasmid pYH3 contains the promoter for T7 RNA polymerase, followed by the *ermC* *Hin*dIII-*Cla*I fragment from pSD155 that replced the *Hin*dIII-*Acc*I fragment of pIBI31. The *Eco*RV-*Bam*HI *ermC* fragment of pYH3 was cloned into M13mp19 that was digested with *Sma*I and *Bam*HI. The *E.coli* strain harboring this M13 phage was EE60. The single-stranded M13 phage DNA from EE60 was the

template for synthesis of the linear RNA-DNA joint molecules (see Section 2-7). This ssDNA was also used as the template to create a *Kpn*I site at the +18 position by oligonucleotide-directed mutagenesis. M13 phage DNA carried in *E. coli* strain EE61 was identical to that in EE60, except in EE61 there was a unique *Kpn*I site in the M13 phage DNA. The pYH3 derivative that contained this *Kpn*I site at the +18 position was pYH4.

2-4 Analysis of RNA

RNA isolation and Northern blot analysis were performed as described (Bechhofer and Dubnau, 1987). Parallel cultures of *B. subtilis* strain carrying the *ermC* gene were grown in minimal medium in the absence of Em to the mid-logarithmic stage of growth. Em (0.02 μg/ml) was added to one of the cultures. Induction was allowed to proceed for 15 min, at which time rifampin was added to 150 μg/ml. One-ml samples were withdrawn at various times after addition of rifampin and were added to 0.5 ml of ice-cold 50 mM NaN_3. Total nucleic acid was first isolated as described (Ulmanen et al., 1985), and then treated with 18 U of RNase-free DNase (Boehringer Mannheim Biochemicals). RNA concentration was measured by OD 260/280. For RNA gels, the amount of total RNA per lane (approximately 3 μg) varied by less than 20%, as judged by ethidium bromide staining and visualization of rRNA bands under UV light. Hybridization was performed at 37°C overnight and the filters were washed at 50°C. The *ermC* 5' end probe is an M13mp19 derivative that contains the the sequences between *ermC* 5'-proximal *Mbo*I and *ermC Hae*III (see Fig. 3). This bacteriophage ssDNA was

labeled by the reverse-priming method (Hu and Messing, 1982), with the following modifications: the primer and template were heated to 90°C for 3 min, kept at 65°C for 10 min, and then cooled to room temperature; NaCl was omitted from the extension reaction; the probe was passed through a Sephadex G-50 column to separate unincorporated nucleotides. In control experiments, the standard concentration of ssDNA probe was in excess of the concentration of *ermC* mRNA, for at least 45 μg of total RNA.

Quantitation of mRNA half-lives was performed by analyzing autoradiograms of Northern blots on a densitometer (Ultroscan XL; LKB Instruments, Inc.).

Reverse transcriptase analysis was performed essentially as described (Graves and Rabinowitz, 1986). The oligonucleotide primer for these experiments was "fragment 2" of Narayanan and Dubnau (1987). A total of 50 μg of RNA was denatured at 65°C for 10 minutes in a 14 μl volume containing 50 mM Tris-HCl (pH 8.0), 8 mM $MgCl_2$, 30 mM KCl, 1 mM dithiothreitol, 4ng of end-labeled primer, and 25 U of RNase inhibitor (Boehringer Mannheim Biochemicals). After an additional 4 minutes at 42°C, deoxynucleoside triphospates (final concentration, 0.5 mM) and 12 Units of avian myeloblastosis virus reverse transcriptase (Life Sciences, Inc.) were added, and incubation was continued at 42°C for 35 minutes. The reaction was stopped by the addition of EDTA (50 mM) and extracted with an equal volume of phenol-chloroform (1:1). Nucleic acid was precipitated by adding 0.5 volume of 6M ammonium acetate and two volumes of ethanol. The dry pellet was suspended in 6μl of water and 4 μl of DNA sequencing dye mix (90% deionized

formamide containing 0.1% bromophenol blue and 0.1% xylene cyanole FF in half-strengh Tris-borate-EDTA buffer [Maniatis et al., 1982]), heated to 80°C for 2 minutes, and run on an 8% polyacrylamide-8M urea sequencing gel. The same primer (unlabeled) was used for dideoxy sequencing of a single-stranded DNA template containing the *ermC* coding strand.

Mapping of *ermC* mRNA decay intermediates with S1 nuclease was performed as described (Berk and Sharp, 1977). The DNA fragments for use as probes in S1 nuclease mapping experiments were the *Bam*HI-*Bcl*I and *Bam*HI-*Hin*dIII fragments from pBD158, which is the high copy version of pBD362. The pBD158 plasmid DNA was digested with *Bcl*I or *Hin*dIII, then treated with calf intestine alkaline phosphatase (Promega Corp.), The *Bcl*I or *Hin*dIII end was labeled with [γ-^{32}P]ATP (Dupont, NEN Research Products) by T4 polynucleotide kinase (Boehringer Mannheim Biochemicals). The 5'-end labeled *Bcl*I or *Hin*dIII fragments were digested with *Bam*HI and the 1,270-bp *Bam*I-*Bcl*I fragment and the 900-bp *Bam*HI-*Hin*dIII fragment were isolated by adsorption to glassmilk (Bio 101, Inc.). The specific activity of DNA probes was 1 x 10^5 to 5 x 10^5 (Cerenkov counts)/min/µg. Total cellular RNA (50µg) was hybridized with 5'-end labeled probe in 10 µl of hybridization buffer containing 40 mM PIPES buffer (Sigma), pH 6.4, 400 mM NaCl, 1 mM EDTA, and 80% (v/v) formamide at 40°C. After hybridization overnight, 200 µl of digestion buffer containing 250 mM NaCl, 40 mM NaOAc, pH 5.5, 1 mM $ZnCl_2$, and 20 µg/ml of denatured calf thymus DNA (Sigma type I) were added and digested with 200 U of S1 nuclease (Boehringer Mannheim Biochemicals) at 37°C for 30 minutes. After the S1

nuclease digestion, 4 µl of 10% sodium dodecyl sulfate, 20 µl of 0.2 M EDTA, and 25 µl of 3 M NaOAc (pH 8.0) were added to stop the reaction. The resultant mixture was extracted with an equal volume of phenol-chloroform (1:1). Two volumes of ethanol were added to the aqueous phase to precipitate the nucleic acids, The dry samples were suspended in 6 µl of TE and mixed with 4 µl of DNA sequencing dye mix, heated to 80°C and run on a 6% polyacrylamide-8M urea sequencing gel. Chemical cleavage of the same probe by the Maxam-Gilbert method (1980) was used for a sequence ladder.

2-5 Preparation of cell extracts

Figure 10 outlines the scheme employed to prepare *B. subtilis* extracts. *B. subtilis* strain BE8 were grown at 32°C overnight in YTP with 5 µg/ml Cm. YTP contained 2.5% tryptose (Difco), 2% yeast extract (Difco), 0.3% K_2HPO_4, and 3% glucose. The culture was diluted in YTP (1:100) and grown with vigorous aeration at 37°C to late-logarithmic phase (320 Klett units). The culture was chilled thoroughly in a slurry of water and ice and harvested by centrifugation at 4°C in a Sorvall GSA rotor for 10 min at 5,000 rpm. The cells were washed with cold AKD buffer (10 mM Tris OAc [pH 8.0],15 mM $Mg(OAc)_2$, 60 mM KOAc, 1 mM dithiothreitol, and 0.20 mM phenylmethylsulfonyl fluoride). Approximately 15 g of cells were suspended in 30 ml of cold AKD buffer supplemented with glycerol to 10% (vol/vol). Cells were disrupted by two passages through a precooled Aminco French pressure cell at 12,000 lb/in^2. Extracts were centrifuged in a Sorvall GSA rotor at 30,000 x g for 30 min, yielding the pellet (P-30) and the supernatant (S-30). The

resultant supernatant (S-30) was recentrifuged in a Ti60 rotor for 60 min at 100,000 x g, yielding the pellet (P-100) and the supernatant (S-100). All the extract fractions (S-30, P-30, S-100 and P-100) were frozen and stored at -135°C in 0.3 ml aliquots.

2-6 Preparation of RNA substrates

Plasmids pYH3 or pYH4 were digested for use in the in vitro transcription reaction. Transcription reactions contained 3 μg of linearized plasmid DNA and 100 U of T7 RNA polymerase in 100 μl of 40 mM Tris-HCl (pH 8.0), 6 mM $MgCl_2$, 2 mM spermidine, 10 mM dithiothreitol, and 100 U RNase inhibitor. Unlabeled ribonucleotides (GTP, ATP and CTP) were present at 500 μM and α-^{32}P-labeled UTP was present at 12 μM. After incubation at 37°C for 2 hr, 3 U of RNase-free DNase (Promega Corp.) were added to reaction mixtures and incubation continued at 37°C for 15 min. Reaction mixtures were extracted with phenol-chloroform (1:1) twice, precipitated with ethanol, washed with 70% ethanol, and finally dissolved in TE buffer (10mM Tris-HCl [pH 8.0] and 1 mM EDTA). For the runoff transcripts used as RNA primers (see Section 2-7), the RNA was synthesized in the presence of 500 μM four ribonucleotides (GTP, ATP, CTP and UTP). The RNA bands detected by ethidium bromide staining were isolated according to the Bio 101 RNaid Kit protocol (Bio 101, Inc.). The isolated RNA was stored at -20°C and could be frozen and thawed several times without apparent degradation.

2-7 Preparation of RNA-DNA joint molecules

Figure 12 outlines the scheme employed to construct RNA-DNA joint molecules. pYH3 DNA was linearized with *Sal*I and used as a template to transcribe a 101-nt RNA (see Section 2-6). This RNA was annealed to EE60 ssDNA in buffer containing 50 mM Tris-HCl (pH 7.5), 300 mM NaCl, and 1 mM EDTA by heating at 90°C for 3 min, keeping at 65°C for 10 min and then cooling to room temperature. DNA extension was performed at 25°C with 10 U of Sequenase Version 2.0 (United State Biochemicals) in 60 µl of 40 mM Tris-HCl (pH 7.5), 20 mM $MgCl_2$, 50 mM NaCl, and 10 mM dithiothreitol. Unlabeled deoxyribonucleotides (dGTP, dCTP and dTTP) were present at 50 µM, and the extension reaction was pulsed at 0°C for 10 min in the presence of 0.16 µM [α-^{32}P]dATP and chased at 37°C for 10 min in the presence of 10 µM unlabeled dATP. After chase, the reaction mixture was extracted with an equal volume of phenol-chloroform (1:1). The RNA-DNA/DNA duplexes were precipitated by adding 0.5 volume of 6M ammonium acetate and two volumes of ethanol. The dry pellet was suspended in water, digested with *Hpa*I at 37°C for 60 min and run on a 1.0% agarose-6.6M formaldehyde gel. The band corresponding to the RNA-DNA joint molecules detected by autoradiography was isolated according to the RNaid Kit protocol (Bio 101, Inc.).

2-8 Preparation of ssDNA substrate

To synthesize the ^{32}P-labeled ssDNA, an M13 "-40" universal sequencing primer was annealed to phage DNA of an M13mp19 derivative which contained a *Sac*I-*Bcl*I fragment of the wild-type

ermC gene cloned between its *Sac*I and *Bam*HI sites. After annealing, dGTP, dCTP and dTTP (final concentration, 50 μM), [α-^{32}P]dATP (0.5 μM), dithiothreitol (5 mM), 10 U of Sequenase Version 2.0, and 10 U of *Hin*dIII were added, and incubated at 37°C for 60 min. The reaction mixture was extracted with an equal volume of phenol-chloroform (1:1), precipitated by adding 0.5 volume of 6M ammonium acetate and two volumes of ethanol. The dried pellet was suspended in 6 μl of TE and 4 μl of DNA sequencing dye mix, heated to 90°C for 3 min and run on a 4% polyacrylamide-8M urea gel. The ssDNA band detected by autoradiography was isolated by adsorption to glassmilk (Bio 101, Inc.).

2-9 Preparation of a circular RNA substrate

To construct circular RNA molecules, I used *Kpn*I-linearized pYH4 to synthesize 5' monophosphoryl 18-nt runoff transcripts as described in Section 2-6, except 2.5 mM GMP was added to the in vitro transcription reaction mixture. The circularization of 5'-monophosphoryl 18-nt RNA molecules was catalyzed by 20 U of T4 RNA ligase (New England Biolabs) in 50 μl of 50 mM Tris-HCl (pH 8.0), 10 mM $MgCl_2$, 2-mercaptoethanol, and 1 mM ATP. After incubation at 37°C for 60 min, the reaction was terminated by boiling for two min and extracted with an equal volume of phenol-chloroform (1:1). RNA was precipitated by adding 0.5 volume of 6M ammonium acetate and two volumes of ethanol, and the dried pellet was suspended in TE.

2-10 Analysis of RNA decay in the *B. subtilis* extracts

Assays of ribonuclease activity were performed at 25°C or 37°C in 10 mM Tris OAc (pH 8.9), 10 mM EDTA, and the appropriate ^{32}P-labeled substrates (prepared as described above). Incubations were initiated by the addition of cell extracts. Samples (30 µl) were removed at various times into an equal volume of phenol, mixed thoroughly, and chilled in ice. After spinning for 3 min at 15,000 x g, 18 µl of the aqueous phase was removed into 9 µl of DNA sequencing dye mix, heated for 3 min at 90°C, quick cooled on ice, and analyzed by electrophoresis on a polyacrylamide gel (29:1 acrylamide:bisacrylamide) with or without 8M urea in Tris-borate-EDTA buffer (Maniatis et al., 1982). Urea-containing gels were fixed by soaking in 5% methanol and 5% acetic acid. Gels were dried at 80°C under vacuum (except for 20% polyacrylamide-8M urea gel), and exposed to X-ray film.

2-11 Digestion of RNA substrates with nucleases

To confirm that the 5' segment of the RNA-DNA joint molecule contains RNA moiety, the isolated 700-nt RNA-DNA joint molecule and 400-nt ssDNA were incubated with 1 µg of DNase-free pancreatic RNase (Boehringer Mannheim Biochemicals) at 37°C. Samples (30 µl) were removed into an equal volume of phenol at 0 and 20 min, and analyzed as described in section 2-10.

The 700-nt RNA-DNA joint molecule and 400-nt ssDNA molecule were incubated with 35 U of RNase-free DNase (Boehringer Mannheim Biochemicals) in buffer containing 100 mM NaOAc, pH 5.0 and 5 mM $MgSO_4$. After incubation at 37°C for 0 min and 30 min,

aliquots (30 µl) of each sample were removed and analyzed as described in Section 2-10.

Linear or circularized RNAs were incubated with 1 µg of DNase-free pancreatic RNase (Boehringer Mannheim Biochemicals) at 37°C. After incubation at 37°C for 0 min and 30 min, aliquots (30 µl) of each sample were removed and analyzed as described in Section 2-10.

Linear or circularized RNAs were incubated with 0.3 U of polynucleotide phosphorylase from *Micrococcus luteus* (Boehringer Mannheim Biochemicals) in buffer containing 50 mM Tris-HCl (pH 8.0), 5 mM $MgCl_2$, 60 mM NaCl, and 10 mM K_2HPO_4. After incubation at 37°C for 0 min and 30 min, aliquots (30 µl) of each sample were removed and analyzed as described in Section 2-10.

CHAPTER THREE

RESULTS

3-1 Construction of a mutant in which SD1 is distal from the 5' end of *ermC* mRNA

One of my thesis projects was to test whether the 5' end of *ermC* mRNA was the target for initiation of decay in *B. subtilis*. If *ermC* mRNA is degraded from the 5' end and the decay is blocked by the presence of a ribosome stalled at the leader peptide ribosome-binding site (SD1), then positioning of SD1 far downstream of the 5' end would allow detection of a differential stability of RNA sequences upstream and downstream of the ribosome stall site.

To address this point, I used plasmid pSD100, which was previously constructed (Fig. 3). A synthetic 30-base-pair fragment with *Sac*I ends was inserted into the *ermC Sac*I site, which is located between the -35 and -10 *ermC* promoter sequences. The 30-bp insert restored the native *ermC* promoter sequences (see Section 2-3) and contained a new *Pvu*II site, which was used to clone isolated *Alu*I fragments from plasmid pC194. One clone was selected that contained a tandem insert of a 275-bp *Alu*I fragment in the *Pvu*II site, yielding plasmid pSD100. Based on its nucleotide sequence (nucleotides 2711 to 2437 of pC194 [Horinouchi and Weisblum, 1982]), this inserted fragment did not appear to contain any transcriptional or translational signals that could complicate the analysis. SD1 was located 580 nucleotides downstream of transcriptional start site in pSD100-encoded *ermC* mRNA.

Figure 3. Construction of pSD100 and derivatives.

The *ermC* gene is represented by the solid bar at the top. Single letters denote relevant restriction endonuclease sites (A, *Alu*I; B, *Bcl*I; C, *Cla*I; H, *Hae*III; M, *Mbo*I; P, *Pvu*II; S, *Sac*I; T, *Taq*I). The *ermC* promoter is indicated by -35 and -10 at the left; transcription terminates upstream of the *Cla*I site (Gryczan et al., 1980; D. H. Bechhofer, unpublished data). The open box in the second line indicates the synthetic 30-base-pair(bp) fragment containing a *Pvu*II site, which was cloned into the *Sac*I site. The hatched bar in pSD100 indicates the 550-bp insert consisting of tandem 275-bp *Alu*I fragment; the 550-bp insert was cloned into the *Pvu*II site. The triangle above the diagram of pSD125 denotes the BAL-31-generrated 25-bp deletion of pSD100. Construction of pSD132 is described in the Section 2-3. The location of the 5' end probe, which was used in Northern blot experiments, is shown at the lower right.

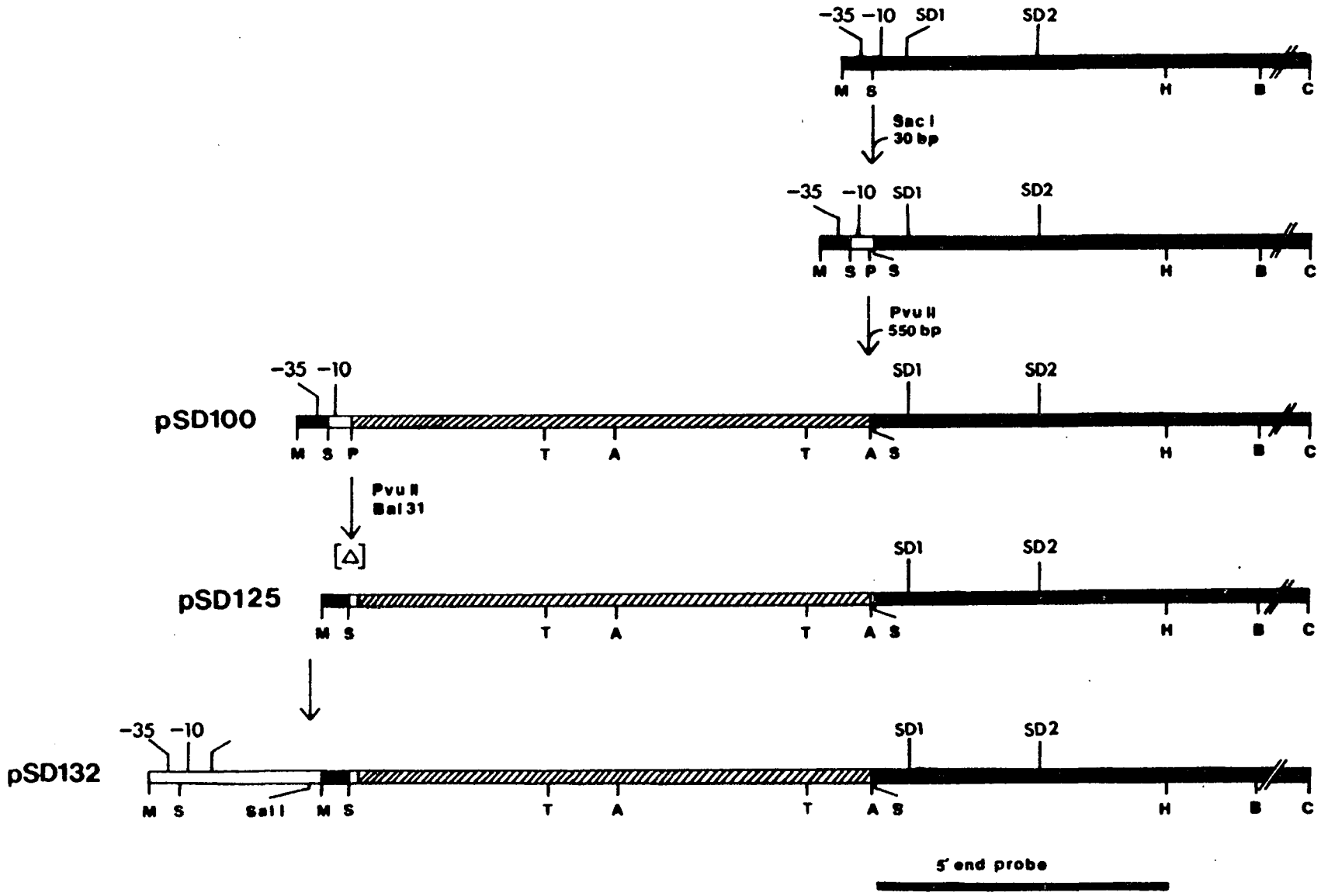
-35
-10
SD1
SD2
M S H B C
Sac I
30 bp
M S P S
Pvu II
550 bp
pSD100
T A T A S
Pvu II
Bal 31
[Δ]
pSD125
pSD132
Sal I
5' end probe

The minicell system of *B. subtilis* was employed to study the induction of methylase expression from plasmid pSD100. Earlier studies have demonstrated that bacteriophage and plasmid DNA can be transcribed and translated in *B. subtilis* minicells (Reeve and Cornett, 1975; Shivakumar et al., 1979). Minicells were isolated from a minicell-producing strain of *B. subtilis* transformed with pSD100. When these minicells were incubated with [^{3}H]leucine in the presence and absence of Em, polypeptides encoded by pSD100 were synthesized and ^{3}H-labeled. As can be seen from Fig. 4A, methylase expression from pSD100 was inducible by Em, indicating that ribosome stalling occurs normally in this construct.

3-2 Analysis of pSD100-encoded *ermC* mRNA

RNA was isolated from a strain containing pSD100 in the presence and absence of Em at various time after rifampin addition (Fig. 4B). The probe, which was complementary to sequences downstream of the *ermC*-proximal *Sac*I site ("5' end probe", see Fig. 3), detected a 1,400-nt (large) RNA and a 900-nt (small) RNA at the time of addition of rifampin. Both of these RNAs were unstable in the absence of Em. In the presence of Em, however, the large RNA was unstable, while the small RNA, which was similar in size to the wild-type *ermC* mRNA, was relatively stable. The reason why the half-life of the small RNA (8 min, as determined by densitometry scanning on lightly exposed autoradiogram) is shorter than the wild-type *ermC* mRNA (40 min) will be explained in Section 4-1. At the zero time point after rifampin addition, the probe also detected unstable RNA fragments of intermediate size.

Figure 4. Analysis of pSD100-encoded polypeptides and RNA.

(A) Minicell analysis of pSD100-encoded polypeptides in the absence (-) and presence (+) of erythromycin (Em). Plasmid pBD142 contains the wild-type *ermC* gene. Both plasmids encode chloramphenicol acetyltransferase (cat), which served as a control for plasmid-specified protein synthesis. (B) Blot analysis of RNA from a strain carrying pSD100 in the presence and absence of Em. The time (in minutes) after rifampin addition is indicated above each lane. Lane A contains RNA from a strain carrying wild-type *ermC* and serves as marker for the migration of *ermC*-sized RNA. Numbers indicate the approximate sizes (in nucleotides) of the RNAs. The cartoon at the left depicts the large RNA with the *ermC* leader stem-loop structure in the uninduced (-Em) conformation. The cartoons at the right depict the large and small induced (+Em) RNAs with the *ermC* leader in the induced conformation. (C) Blot analysis of RNA isolated from a strain carrying plasmid pSD125 (lane C), the pSD100 derivative from which the upstream promoter was deleted. RNA was probed with either the 5' end probe (left) or a probe for pC194 cat mRNA (right). Plasmid pSD125 carries the pC194 cat gene. As a control for plasmid-specified RNA, total RNA from a strain carrying pC194 (encodes cat but not *ermC*; lanes A) or pE194 (encodes *ermC* but not cat; lanes B) was included on the blots.

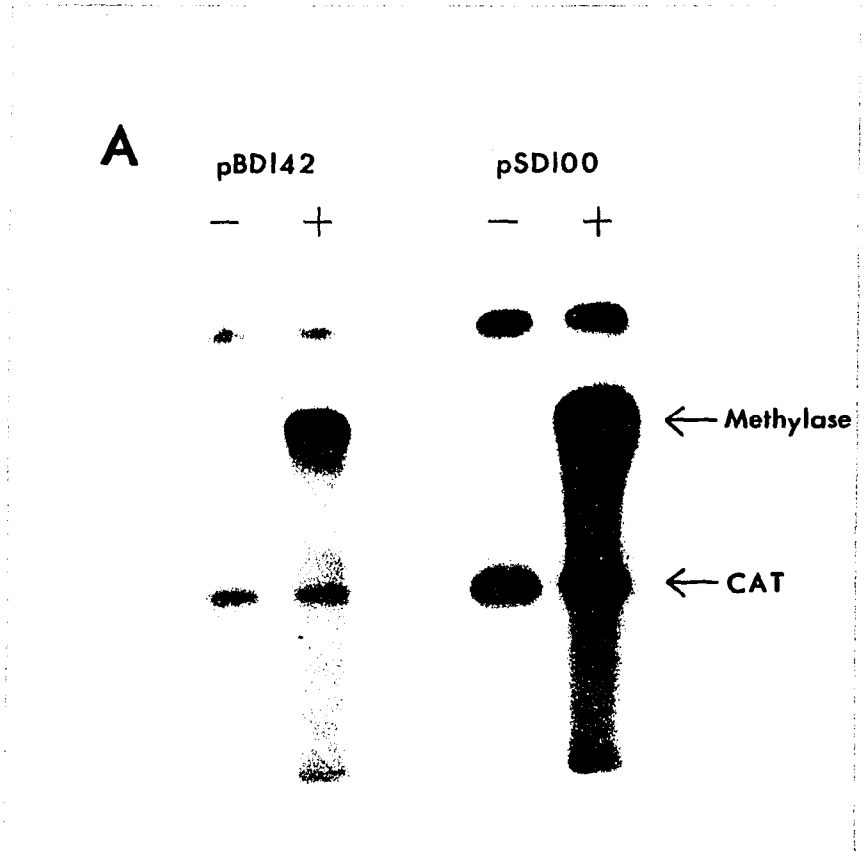
A
pBD142
pSD100
−
+
−
+
Methylase
CAT

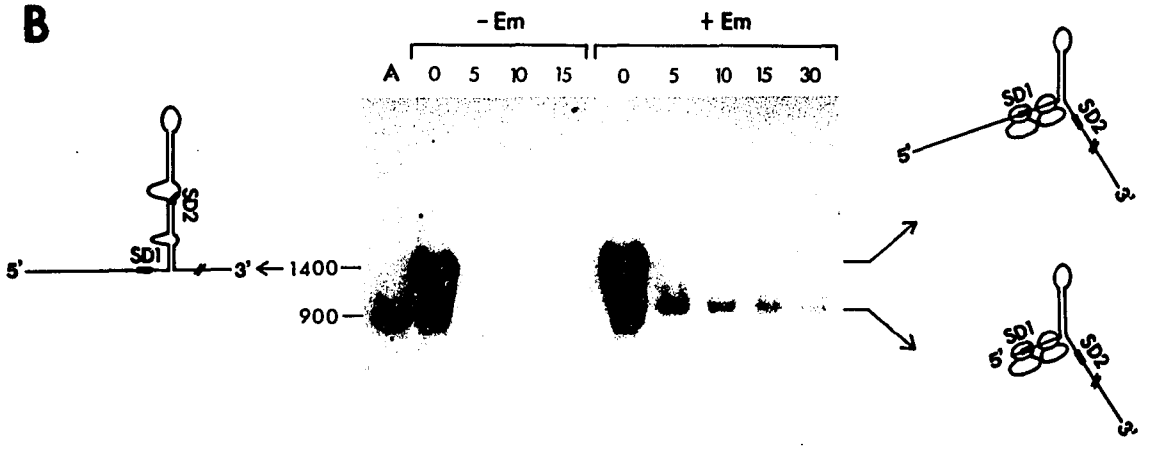
B
- Em
+ Em
A 0 5 10 15 0 5 10 15 30
SD2
SD1
5'
3'
1400
900
SD1
SD2
5'
3'
SD1
SD2
5'
3'

C

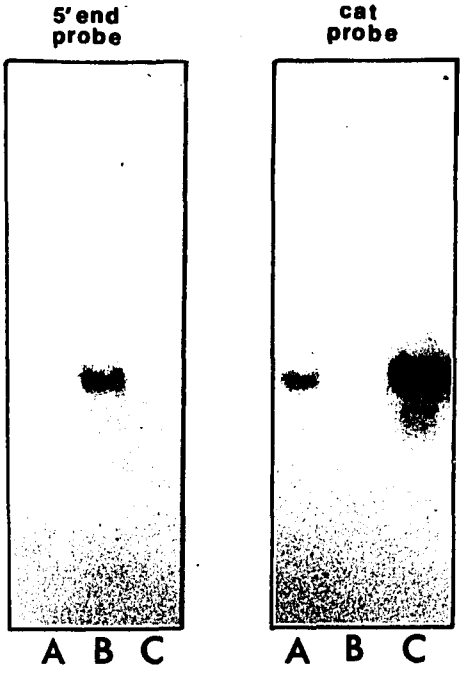

To demonstrate that the small RNA was a processed product of the large RNA and was not transcribed from a promoter within the 550-bp insert, RNA from the a strain carrying pSD100 was probed with DNA complementary to the inserted *Alu*I fragment. Only the large RNA was detected by this upstream probe, indicating that the small RNA is not transcribed from a promoter within the inserted DNA (data not shown). In addition, the promoter for the large RNA was inactivated by a BAL-31 deletion from the *Pvu*II site, which removed 15 nucleotides upstream and 10 nucleotides downstream of the *Pvu*II site (pSD125, Fig. 3). The RNA encoded by the BAL-31 deletion plasmid was probed with the 5' end probe (Fig. 4C). Neither the large nor the small RNA was detected by the *ermC* probe, demonstrating that the small RNA was not transcribed from a different promoter. Therefore, the small RNA must be a processed product of the large RNA.

An unstable large RNA and a stable small RNA in the presence of Em could be explained if the 5' end of *ermC* mRNA is the initiation site for decay. In the presence of Em, there is a backup of stalled ribosomes from the leader peptide sequence to SD1, which is located 580 nucleotides downsream of the 5' end of pSD100-encoded *ermC* mRNA. A ribonuclease, possibly a 5'-to-3' exoribonuclease or an endoribonuclease that binds at the 5' end and tracks in the 5'-to-3' direction, attacks the unprotected 5' end and degrades this mRNA up to the site of the stalled ribosome, producing the small RNA. If this model is correct, then any RNA having an internal ribosome stall site should be processed in the same way as pSD100-encoded *ermC*

mRNA. To test this, RNA encoded by a construct that had a different sequence upstream of the *ermC* ribosome stall site was analyzed.

Plasmid pBD362 is a low-copy version of pBD158, which was constructed previously ("deletion 14" of Hahn et al., 1982). In pBD362, *ermC* is transcribed from a promoter located approximately 1,100 nucleotides upstream of SD1. These 1,100 nucleotides are derived from pUB110 and pC194 DNA and are not related to the pC194 DNA that constituted the 550-nt insert in pSD100. Methylase synthesis in a strain carrying pBD362 is inducible by Em, so that ribosome stalling occurs normally in this construct. RNA was isolated from a strain containing pBD362 and probed with the 5' end probe. An unstable, large (2,000-nt) RNA and a small (900-nt) RNA that was relatively stable (5-min half-life) in the presence of Em were detected (Bechhofer and Zen, 1989). This small RNA was similar in size to wild-type *ermC* mRNA, as was the small RNA from a strain carrying pSD100. Thus, in the presence of Em, pSD100-encoded and pBD362-encoded large RNAs, which contained different nucleotide sequences upstream of the ribosome stall site, are processed to yield similarly sized small RNAs.

3-3 Mapping the 5' ends of the processed small RNAs

Reverse transcriptase analysis was used to map the 5' ends of the small RNAs that were detected by Northern blot analysis. RNA isolated from pSD100- and pBD362-containing strains at 10 min after rifampin addition in the presence of Em was used as a template for a 5' end-labeled oligonucleotide that was complementary to the leader peptide coding sequence. The data presented in Figure 5 reveal that

Figure 5. Reverse transcriptase mapping of stable, small RNAs.

Reverse transcripase was used to extend an oligonucleotide primer annealed to the *ermC* leader peptide sequence. RNA was isolated from a strain containing wild-type *ermC* (lane 1) and from strains carrying plasmid pSD100 (lane 2) and plasmid pBD362 (lane 3) at 10 min after rifampin addition in the presence of Em. The four left lanes are a dideoxy sequencing ladder of the *ermC* leader region with the same oligonucleotide primer as was used in the reverse transcriptase reactions. The template for the sequencing reactions was M13 ssDNA containing the coding strand of the *Mbo*I-*Bcl*I fragment from pSD100 (see Fig. 3). The arrow marks the positions of the 5' ends of pSD100 and pBD362 RNAs, which were 57 to 58 nucleotides upstream of SD1.

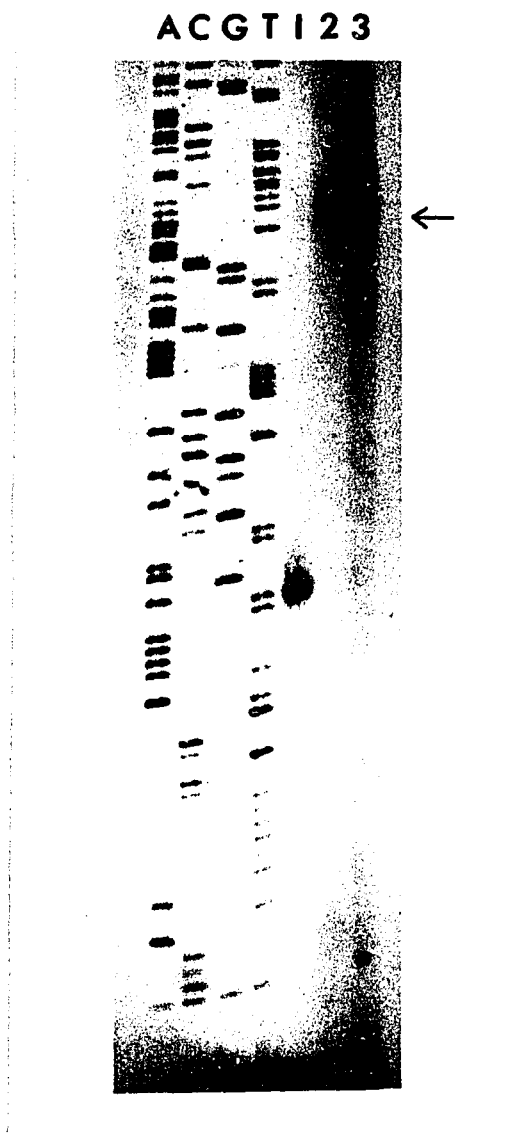
ACGTI23

the 5' ends of the stable, small RNAs mapped to the same site, which was 57 to 58 nucleotide upstream of SD1. The fact that the 5' ends of both small RNAs were the same distance from SD1, even though the sequences upstream of SD1 in pSD100 and pBD362 were different, fits well with our working hypothesis. A sequence-independent degradation of the large RNAs begins at the 5' end and continues downstream until its progress is blocked by a stalled ribosome.

The appearance of the small RNAs could also be explained by endonucleolytic cleavage that does not require initiation at the 5' end. Two modes of endonucleolytic attack that could account for the presence of stable, small RNAs that are processed products of the unstable large RNA were considered: (i) nonspecific endonucleolytic cleavages in the upstream sequence, followed by 3'-to-5' exonucleolytic decay, and (ii) specific endonucleolytic cleavage at the site 57 to 58 nucleotides from SD1, followed by rapid 3'-to-5' exonucleolytic decay of the upstream RNA. Although the sequences at that site were different in pSD100 and pBD362, it was possible that the presence of a stalled ribosome triggered an endonucleolytic cleavage adjacent to it. The experiment described in the next section was designed to eliminate these two possibilities.

3-4 An RNA with 5' terminal and internal ribosome stall sites

To prove that the small RNA was generated by a ribonucleolytic decay proceeding from the 5' end and not by endonucleolytic cleavage, a derivative of pSD100 that had an additional *ermC* ribosome stall site at the 5' end of the large RNA was

constructed. If the small RNA was generated by endonucleolytic cleavage, then the same pattern (an unstable large RNA and a stable small RNA) should be observed in a strain carrying a plasmid which encodes an RNA that has ribosomes stalled both at the 5' end and internally. However, if the small RNA is the result of decay initiating at the 5' end, then the presence of a stalled ribosome at the 5' end would block this decay and only a large, stable RNA would be observed.

From experiments with deletion mutants in the *ermC* leader region, it has been shown that the leader peptide coding sequence alone, without the entire *ermC* leader stem-loop structure, is sufficient to allow ribosome stalling in the presence of Em (Hue and Bechhofer, 1991). A small DNA fragment that contained the first 90 bp of *ermC*, including SD1 and the leader peptide coding sequence, was cloned upstream of the inserted *Alu*I fragments in pSD100 to yield plasmid pSD132 (Fig. 3; see Section 2-3). Analysis of protein synthesis in minicells containing pSD132 showed that methylase expression was inducible by Em (data not shown), demonstrating that ribosome stalling occurs normally at the internal stall site.

RNA was isolated from a strain carrying pSD132, in the presence and absence of Em. As can be seen from the Northern blot analysis in Fig. 6, in the presence of Em the major RNA species that was detected was the large RNA. This was the full-length RNA which was stable because of the presence of a stalled ribosome at the 5' end. The amount of the large RNA was greater than that of the other RNA species detected (compared with Fig. 4B), a result that was not expected if rapid endonucleolytic processing of the large RNA

Figure 6. Blot analysis of pSD132-encoded RNA.

Plasmid pSD132 encoded an mRNA that contained two ribosome stall sites, one at the 5' end of the message and one internally. The cartoon at the right depicts the induced full-length RNA. Lane A, RNA from a strain carrying pE194 (wild-type *ermC*); lane B and C, RNAs from a strain carrying pSD100, isolated at 0 and 5 min, respectively, after rifampin addition in the presence of Em (see Fig. 4B).

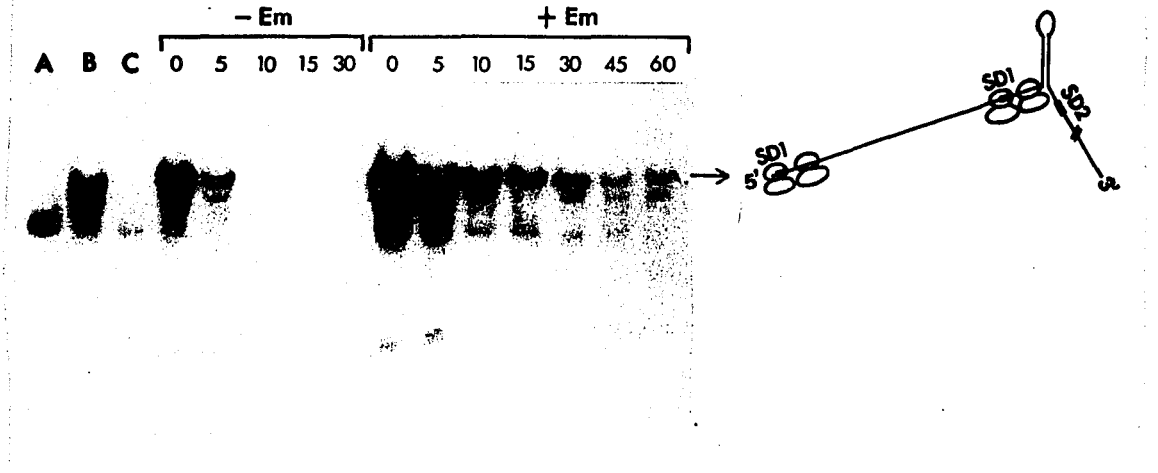
A B C
− Em
0 5 10 15 30
+ Em
0 5 10 15 30 45 60
SD1
5'
SD1
SD2
3'

occurred. This result indicates that the small RNA is generated by a processive decay from the 5' end and not by endonucleolytic cleavage.

3-5 An RNA with two internal ribosome stall sites

From the decay study of an RNA with an internal ribosome stall site (pSD100 and pBD362), we showed that ribosome stalling provides stability to sequences downstream but not upstream of the message. According to our hypothesis that *ermC* mRNA is degraded by a processive 5'-to-3' exoribonuclease, an RNA with two internal ribosome stall sites should yield an unstable full-length RNA and two relatively stable decay intermediates since ribosome stalling will occur at two internal leader peptide sequences.

To test this prediction, a plasmid (pSD192) was constructed that encodes an *ermC* mRNA with two internal ribosome stall sites (see Fig. 7A and Section 2-3). In pSD192 *ermC* mRNA is transcribed from an *ermC* promoter located approximately 300 nucleotides upstream of the first ribosome-binding site and leader peptide coding sequence, which are sufficient to allow ribosome stalling in the presence of Em (Section 3-4). In addition to the first ribosome stall site, *ermC* mRNA encoded by pSD192 also contains an *ermC* leader sequence located approximately 600 nucleotides downstream of the first ribosome stall site.

RNA was isolated from a strain carrying pSD192, in the presence and absence of Em. As can be seen from the Northern blot analysis in Fig. 7B, the 5' end probe detected three major RNAs of the predicted sizes: an 1,800-nt (large) RNA, a 1,500-nt (intermediate-

Figure 7. Construction of pSD192 and blot analysis of pSD192-encoded RNA.

(A) Construction of pSD192. pBD452 is a derivative of pBD142 that has a *Sal*I linker inserted 6 nucleotides downstream of the *ermC* leader peptide coding sequence. Single letters denote relevant restriction endonuclease sites (B, *Bcl*I; E, *Eco*RI; H, *Hin*dIII; P, *Pst*I; S, *Sal*I). The *ermC* promoter is indicated by -35 and -10. By oligonucleotide-directed mutagenesis, the *Bgl*II and *Hin*dIII sites were created between -10 and SD1, yielding pSD155. The hatched bar in pSD172 indicates the 470-base-pair(bp) *Sal*I-*Eco*RI fragment derived from pUB110. The solid bar in pSD192 indicates the *Bam*HI-*Hin*dIII 340-bp fragment derived from pUB110, which was cloned between the *Bgl*II and *Hin*dIII sites of pSD172. Plasmid pSD192 encodes an mRNA that contains two internal ribosome stall sites, which are indicated by asterisk (*). (B) Blot analysis of RNA from the strain carrying pSD192 in the presence and absence of Em. The time (in minutes) after rifampin addition is indicated above each lane. Numbers indicate the approximate sizes (nucleotides) of RNAs. Lane A contains RNA from a strain carrying pE194 (wild-type *ermC*) strain and serves as a marker for the migration of *ermC*-sized RNA.

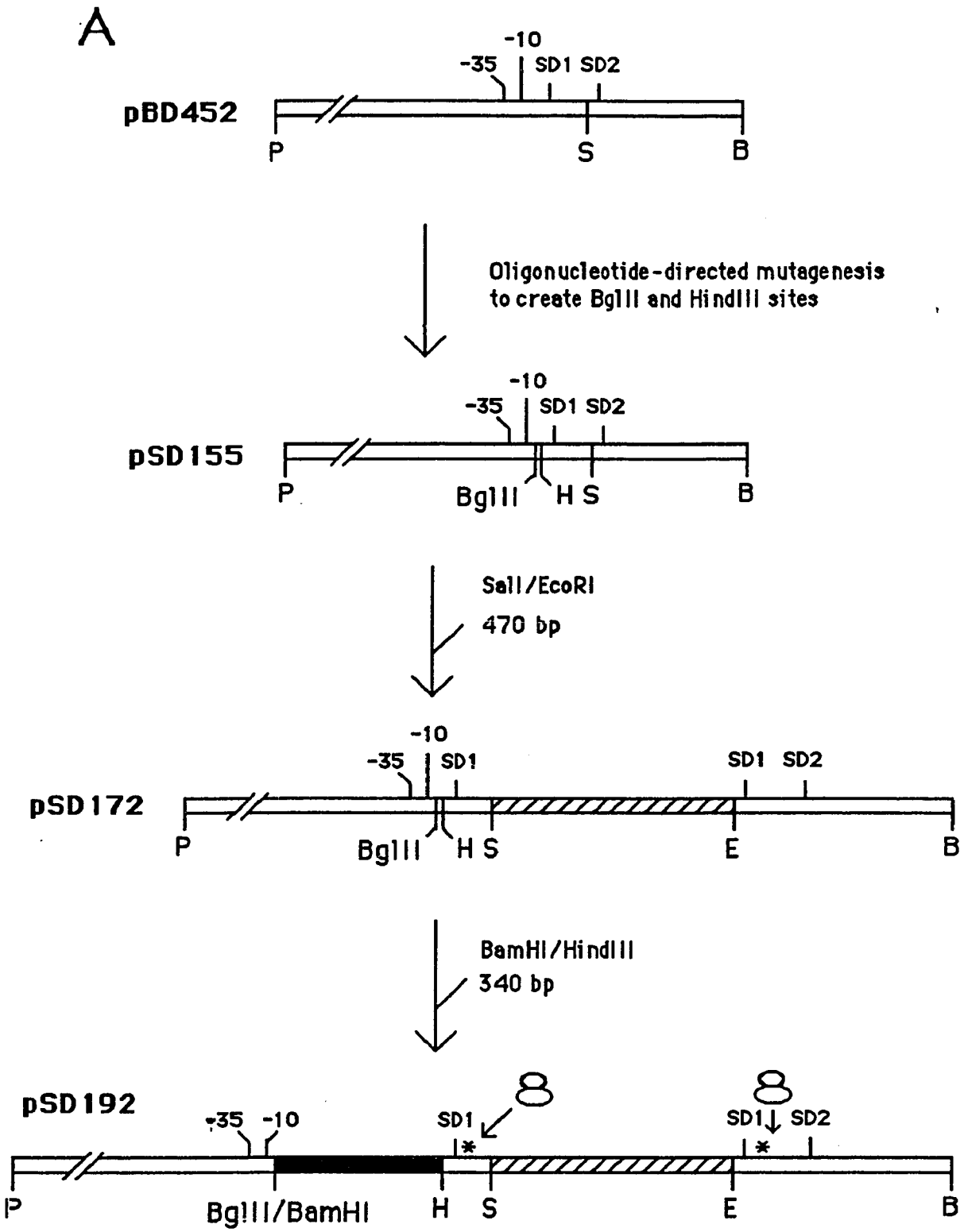
A
pBD452
-10
-35
SD1 SD2
P
S
B
Oligonucleotide-directed mutagenesis
to create BglII and HindIII sites
pSD155
-10
-35
SD1 SD2
P
BglII
H S
B
SalI/EcoRI
470 bp
pSD172
-10
-35
SD1
SD1 SD2
P
BglII
H S
E
B
BamHI/HindIII
340 bp
pSD192
-35
-10
SD1
SD1
SD2
P
BglII/BamHI
H
S
E
B

B

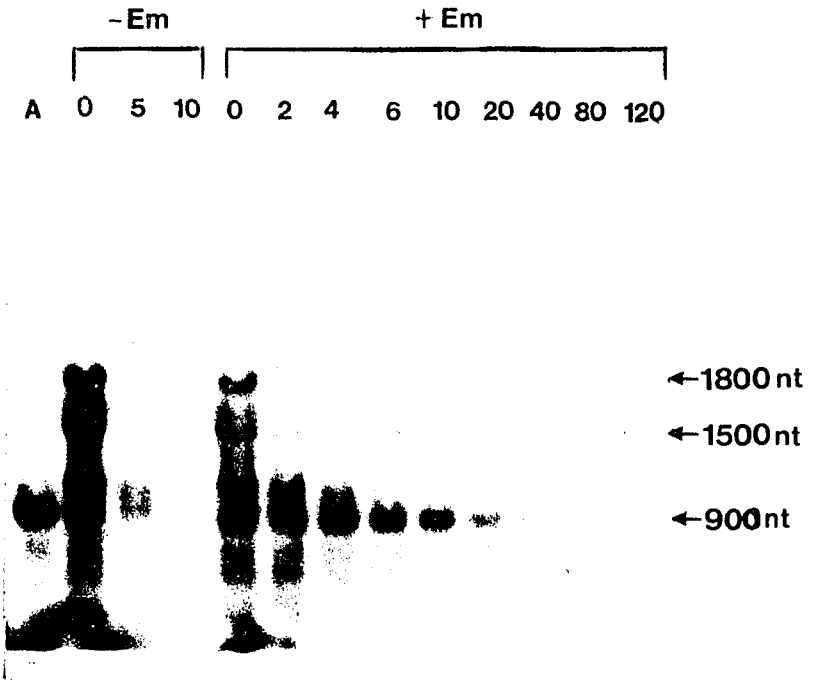

sized) RNA, and a 900-nt (small) RNA. All of these RNAs were unstable in the absence of Em. In the presence of Em, however, the large RNA was very unstable, while the intermediate-sized and small RNAs were relatively stable. Furthermore, shortly after the addition of rifampin, the amount of the small RNA was greater than that of intermediate-sized RNA. The different amount of two relatively stable RNA decay intermediates could be explained by our 5'-to-3' exoribonuclease hypothesis. A processive 5'-to-3' exoribonuclease initiates the degradation of the full-length RNA from the unprotected 5' end but the processive decay is slowed down by the ribosome stalled at the first ribosome stall site, yielding the intermediate-sized RNA. The small RNA is generated by the further decay of the intermediate-sized RNA up to the second ribosome stall site. The accumulation of the small RNA is consistent with the processive 5'-to-3' exoribonuclease hypothesis since the small RNA was the ultimate stable decay intermediate. An 1,100-nt RNA was also detected shortly after rifampin in the absence or presence of Em. If a processive RNase was responsible for the degradation of *ermC* mRNA, then the 1,100-nt RNA could represent pausing at RNase resistance site.

3-6 Mapping the 5' ends of RNA decay intermediates by S1 nuclease analysis

Probing of RNAs encoded by pSD100 and pBD362 revealed, in addition to the prominent large and small RNAs, a smear of unstable intermediate-sized RNAs (Fig. 4B). In the pBD362-containing strain, some RNAs were distinguishable against the background (Bechhofer

and Zen, 1989). Even in the absence of Em, *ermC*-sized mRNAs were detected shortly after rifampin addition. If a processive RNase was responsible for the decay of *ermC* mRNA, then the intermediates detected in the pBD362-containing strain could represent pausing at RNase-resistant sites. The following 5'-end mapping of the decay intermediates by S1 nuclease was designed to understand the nature of RNase pausing. The *ermC*-sized RNA detected at the zero time point in the absence of Em could be explained by RNase pausing at the *ermC* leader stem-loop structure, which is predicted to be very stable (Gryczan et al., 1980). Alternatively, the presence of the *ermC*-sized RNA could be due to the protective effect of ribosomes that load at SD1 and translate the leader peptide coding sequence (without stalling).

Total RNA was isolated from a pBD362-containing strain at 1 and 5 min after rifampin addition in the presence of Em and hybridized to probes that were designed to detect upstream decay products. Samples were digested with S1 nuclease, followed by separation on a denaturing polyacrylamide sequencing gel and autoradiography. The size of the probes, sites of 5'-end labeling, and the protected fragments are shown in Fig. 8D. Due to the resolution of polyacrylamide gel, the 5' end mapping sites are within 3-nt variation. As seen in Fig. 8A and D, three relatively stable protected fragments were detected by using a probe labeled at the *BclI* site. The 5' ends of the major protected fragments detected correspond to the residues 1108, 1197 and 1206 (counting from the transcription start point). The residue 1108 is located 59 nucleotides upstream of SD1, which is consistent with the results obtained by reverse

Figure 8. S1 nuclease mapping of the 5' ends of *ermC* mRNA decay intermediates.

Total RNA was isolated from a strain carrying pBD362 in the presence of Em at various times after the addition of rifampin. The RNA was annealed with a ^{32}P-5'-end-labeled *Bcl*I-*Bam*HI probe (panel A) or *Hin*dIII-*Bam*HI probe (panels B and C) at 40°C, digested with S1 nuclease, and run on a 6% polyacrylamide-8M urea sequencimg gel. (A), (B) and (C) Lanes 1 and 2, RNA isolated at 1 and 5 min, respectively, after the addition of rifampin. Lane 3, probe not digested with S1 nuclease. Lane 4, probe digested with S1 nuclease. Sequencing markers, A+G and C+T, are shown in lanes 5 and 6, respectively. The running time of panel C was longer than that of panel B. (D) The probes and protected fragments in relation to the *ermC* gene. The hatched bar indicates the *ermC* transcript, +1 denotes the beginning of transcription, and the numbers indicate the residues of the *ermC* transcript counting from the transcription initiation site. (E) Possible secondary structures of nucleotides 761 to 790 and nucleotides 1030 to 1070 from the pBD362-encoded mRNA.

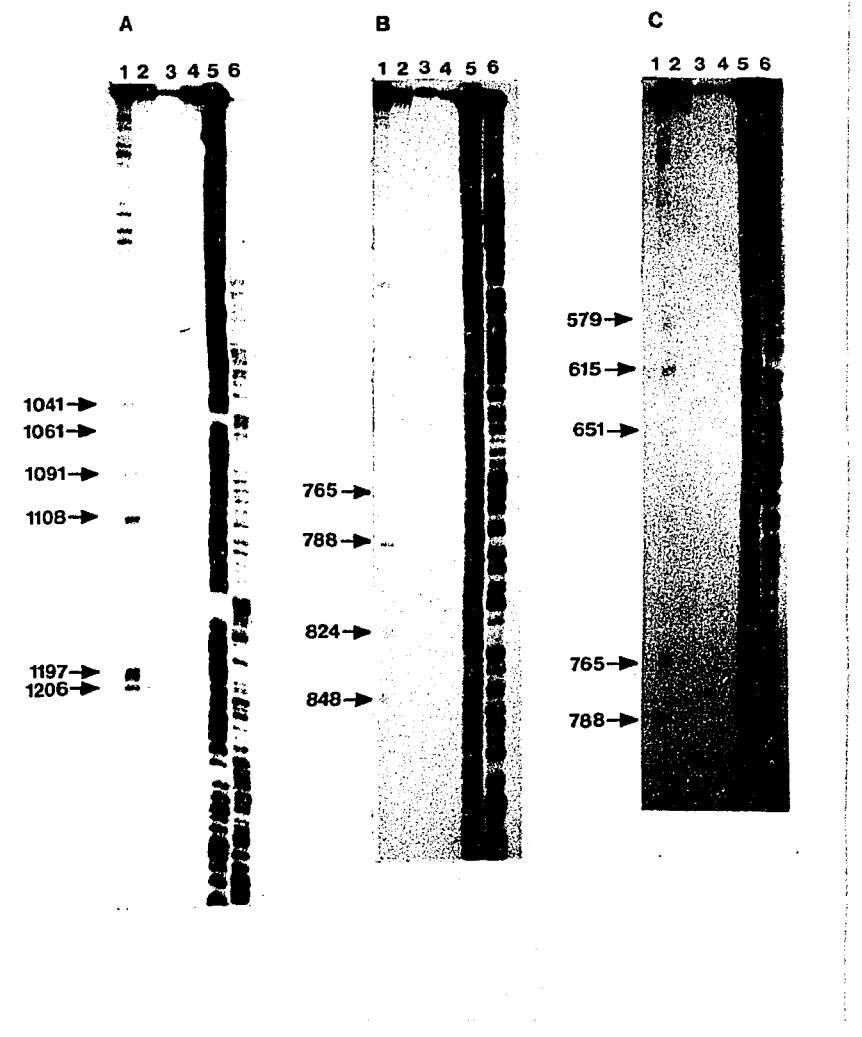
A
1 2 3 4 5 6
1041
1061
1091
1108
1197
1206
B
1 2 3 4 5 6
765
788
824
848
C
1 2 3 4 5 6
579
615
651
765
788

D

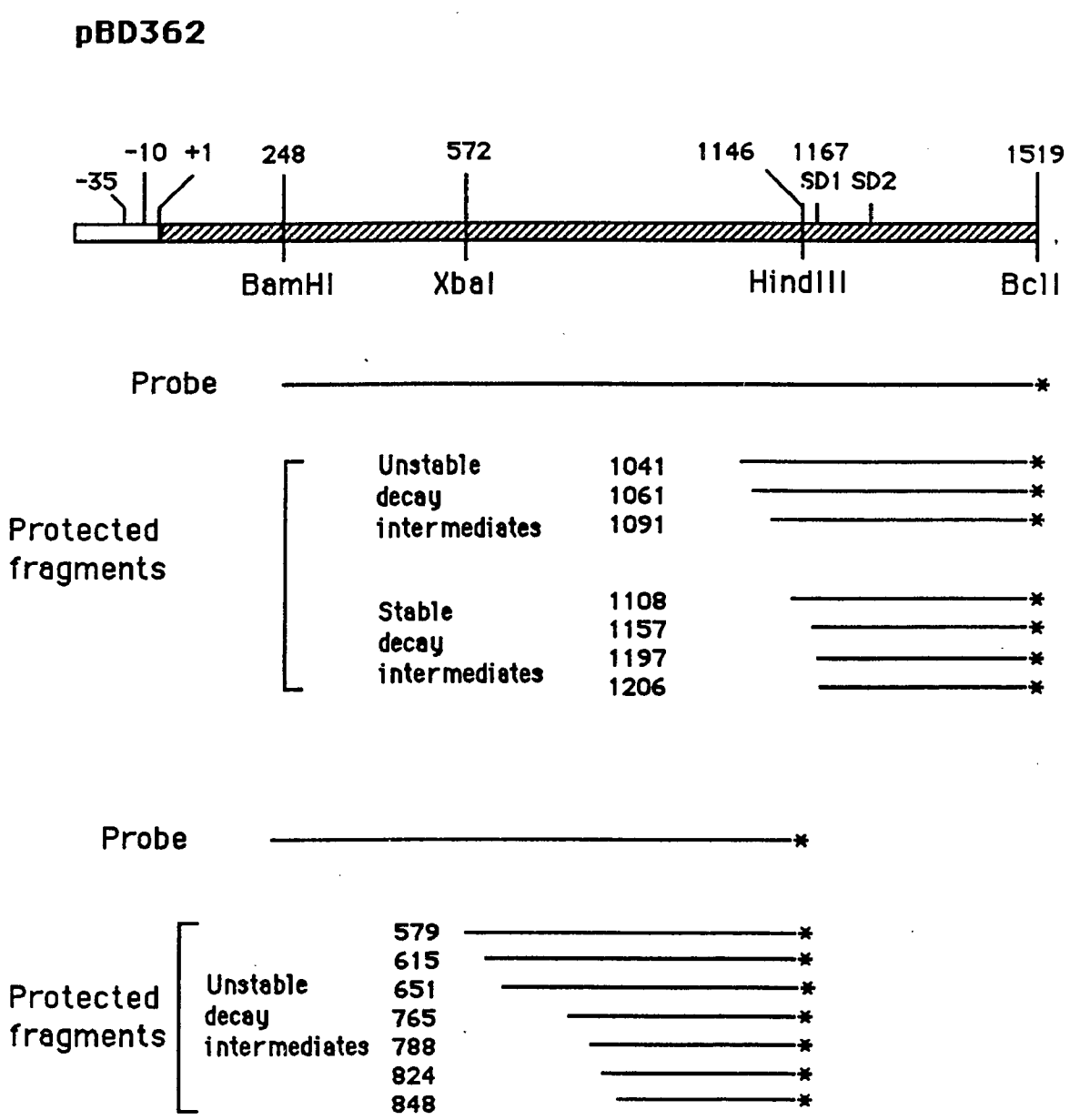
pBD362
-10
+1
248
572
1146
1167
1519
-35
SD1
SD2
BamHI
XbaI
HindIII
BclI
Probe
Protected fragments
Unstable decay intermediates
1041
1061
1091
Stable decay intermediates
1108
1157
1197
1206
Probe
Protected fragments
Unstable decay intermediates
579
615
651
765
788
824
848

E

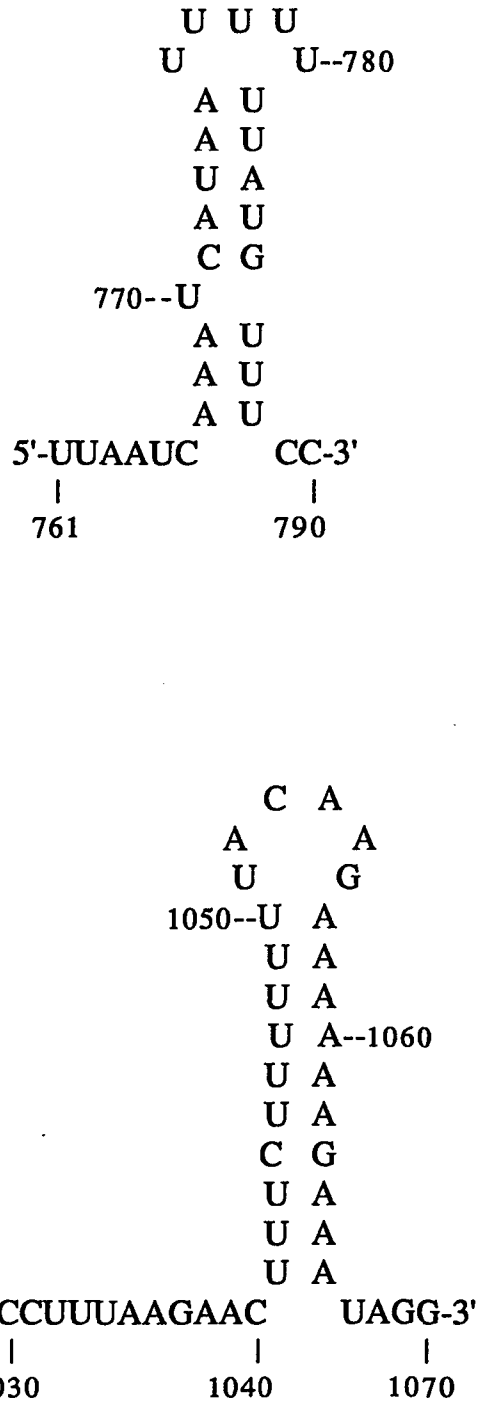
U U U
U U--780
A U
A U
U A
A U
C G
770--U
A U
A U
A U
5'-UUAAUC CC-3'
761 790
C A
A A
U G
1050--U A
U A
U A
U A--1060
U A
U A
C G
U A
U A
U A
5'-CCUUUAAGAAC UAGG-3'
1030 1040 1070

transcriptase analysis of pBD362-encoded *ermC* mRNA (see Fig. 5). The residues 1197 and 1206 correspond to the 7th and 10th amino-acid-coding sequences in the leader peptide sequence. These bands were not observed in Fig. 5 because the primer used in the reverse transcriptase analysis is annealed close to these leader peptide coding sequences, thereby the product of primer extension run off the gel. The 5' ends of these relatively stable RNAs could be due to blockage of the progression of a 5'-to-3' exoribonuclease by Em-bound ribosomes. S1 nuclease mapping of *ermA* mRNA decay intermediates also showed the 5' ends of decay intermediates around the ribosome stall site (Sandler and Weisblum, 1989). According to "two-ribosome stalling" model, a ribosome stalled in the *ermC* leader peptide sequence causes another ribosome, which is loading at SD1, to stall. The ribosome stalled at SD1 slows down the progress of degradation, giving rise to the protected end at residue 1108. We suggest that after the ribosome stalled in the *ermC* leader peptide sequence leaves the message, the following ribosome moves downstream and stalls in the leader peptide sequence. This stalled ribosome could block the progress of an RNase and may give rise to the protected 5' ends at residues 1197 and 1207.

More than ten unstable protected fragments were detected by using a probe labeled at the *Hin*dIII site (Fig. 8B and C) and the 5' ends of ten unstable protected fragments were mapped and shown in Fig. 8D. By using a computer search for possible stem-loop structures (Devereux et al., 1984) that could be involved in protecting downstream sequences from exonucleolytic degradation, 5'-end residues 765 and 1041 of the decay intermediates locate near the 5'-

proximal ends of the predicted stable stem-loop structures (Fig. 8E). However, 5' ends of the other unstable decay intermediates do not correspond to the 5' proximal end of the predicted secondary structure. From S1 nuclease mapping of the stable and unstable decay intermediates, we conclude that the stalled ribosome effectively causes the pausing of a putative 5'-to-3' exoribonuclease, and some secondary structures are also able to cause pausing.

3-7 Preparation of RNA substrates

The in vivo study using a molecular genetics approach has shown that the decay of *ermC* mRNA in *B. subtilis* occurs either by a 5'-to-3' exoribonuclease or by an endoribonuclease that tracks in the 5'-to-3' direction from the 5' end. In order to further confirm this hypothesis, I turned to *B. subtilis* extracts and wished to show this enzymatic activity biochemically.

To prepare a runoff *ermC* transcript, I used plasmid pYH3, which was previously constructed (D. H. Bechhofer, unpublished data). The *Hin*dIII-*Cla*I fragment of pSD155 containing the *ermC* gene was ligated between the *Hin*dIII and *Acc*I sites of pIBI31 to generate pYH3, as illustrated in Fig. 9. Plasmid pYH3 contains the promoter for T7 RNA polymerase followed by the *ermC* leader region and coding sequence. Transcription of *Bam*HI-linearized pYH3 yields an *ermC*-sized transcript (lane 1 in Fig. 11). The body of this RNA is identical to that of the wild-type *ermC* RNA. The 5' end of this in vitro transcript contains 9 additional nucleotides encoded by the vector and *Hin*dIII linker and the 3' end of this runoff transcript contains

Figure 9. Structure of plasmids pYH3 and pYH4.

The *ermC* gene is represented by the hatched bar. The in vitro transcription initiation site is indicated by +1. Single letters denote relevant restriction endonuclease sites (A, *Acc*I; B, *Bam*HI; C, *Cla*I; V, *Eco*RV; H, *Hin*dIII; K, *Kpn*I; S, *Sal*I). To generate pYH3, a *Hin*dIII-*Cla*I fragment of pSD155 containing *ermC* gene was ligated into pIBI31 previously digested with *Hin*dIII and *Acc*I. Plasmid pYH4 contains a *Kpn*I site that was introduced into +18 position by oligonucleotide-directed mutagenesis.

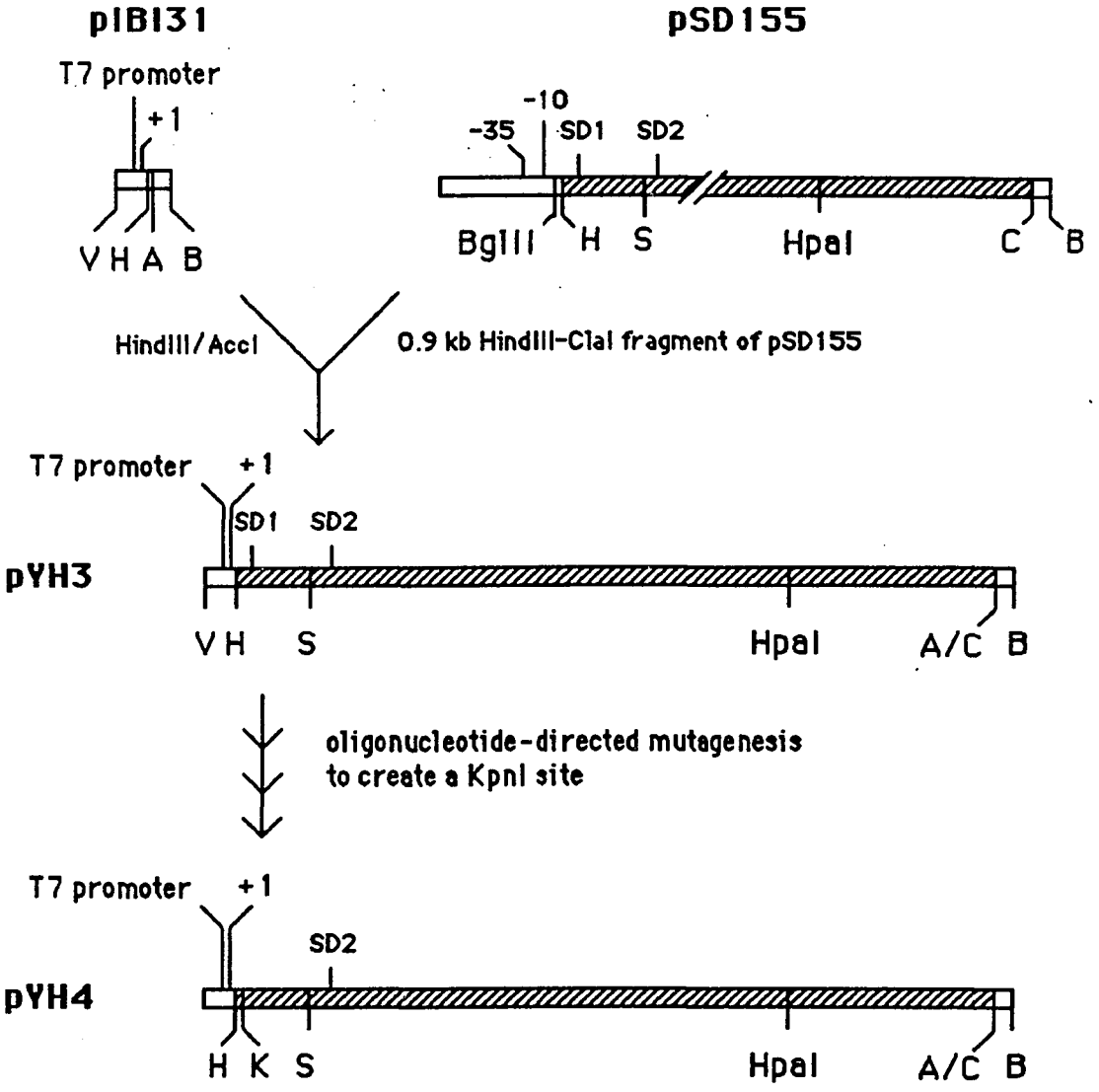

5' sequence of wild-type ermC mRNA

pppAUUUUAUAAGGAGGAAAAAAUAUG----

SD1

5' sequence of mRNA transcribed from pYH3

pppGGGAGAAGCUUUUAUAAGGAGGAAAAAAUAUG----

HindIII SD1

5' Sequence of mRNA transcribed from pYH4

pppGGGAGAAGCUUUUAUAAGGUACCGGAAAAAAUAUG----

HindIII KpnI

50 additional nucleotides past the putative *ermC* transcriptional termination site.

3-8 Degradation of pYH3 *ermC* mRNA in vitro

In order to identify a 5'-to-3' exoribonuclease activity biochemically, *B subtilis* cell extracts were prepared (Fig. 10). *B. subtilis* strain BE8 was chosen for cell extract preparation since it contains plasmid pBD246 which carries an *ermC-lacZ* fusion gene. The assay for β-galactosidase activity was used to monitor protein stability in *B. subtilis* extracts during the preparation and storage of cell extracts. An overnight BE8 culture was diluted 100-fold and grown to late-logarithmic phase. Cells were collected by centrifugation and suspended in AKD buffer. Cells were disrupted by passage through a French press cell. The resultant crude cell extract was clarified at 30,000 x g, yielding the pellet (P-30) and the supernatant (S-30). S-30 was further centrifuged at 100,000 x g, yielding the pellet (P-100) and the supernatant (S-100). Aliquots of S-100 were used for assay of ribonuclease activity.

Transcription of pYH3 linearized with *Bam*HI in the presence of [α-^{32}P]UTP gave an *ermC*-sized RNA labeled with ^{32}P. A time course of incubation with an S-100 extract is shown in Fig. 11. The RNA substrate was degraded within 20 min of incubation. The digestion rate of RNA substrate was dependent on the amount of the S-100 extract added (data not shown). The RNase activity of the S-100 extract at 37°C was better than at 25°C and the optimal pH was between 8.0 and 8.9 (data not shown). Although the RNase activity was also present in the S-30, P-30 and P-100 (data not shown), only

Figure 10. Flow chart of the preparation of *B. subtilis* extracts.

B. subtilis cells were grown to late-logarithmic phase and collected by centrifugation. The cells were resuspended in AKD buffer and passed through a French press cell. The resultant crude extract was centrifuged at 30,000 x g to yield the pellet (P-30) and the supernatant (S-30). The S-30 was centrifuged at 100,000 x g, yielding the pellet (P-100) and the supernatant (S-100).

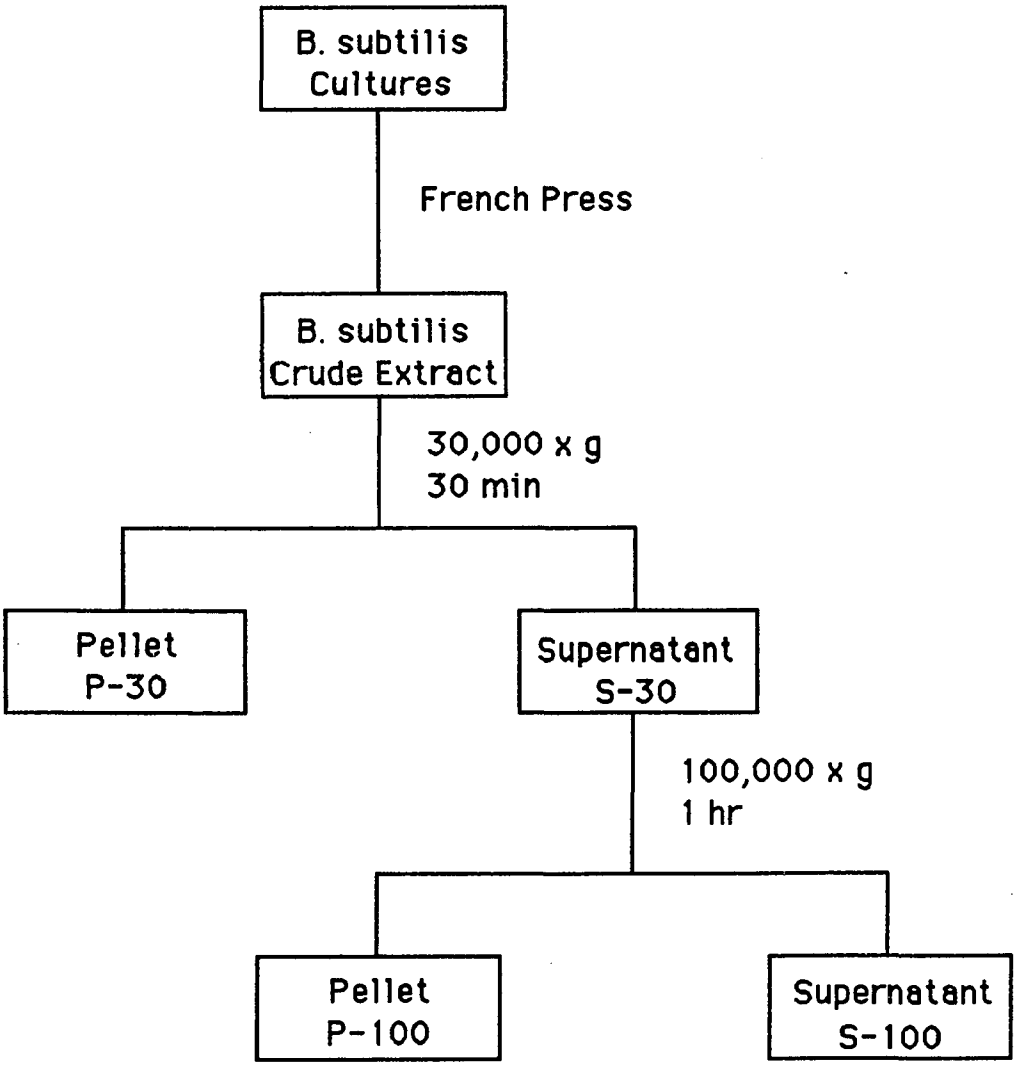
B. subtilis Cultures
French Press
B. subtilis Crude Extract
30,000 x g
30 min
Pellet P-30
Supernatant S-30
100,000 x g
1 hr
Pellet P-100
Supernatant S-100

Figure 11. RNase and DNase activities of the *B. subtilis* extract S-100.

The ^{32}P-labeled 900-nt RNA and 400-nt ssDNA substrates were digested at 25°C with an S-100 extract. Aliquots containing 30 µl of the digest were phenol extracted and analyzed electrophoretically (see Section 2-10). Lane 1: ^{32}P-labeled substrates were incubated without extract. Lanes 2 and 4: ^{32}P-labeled substrates were incubated with an S-100 extract for 20 min at pH 8.9 and at pH 8.0. Lanes 3 and 5: ^{32}P-labeled substrates were incubated with an S-100 extract for 20 min in the presence of 10 mM EDTA at pH 8.9 and at pH 8.0.

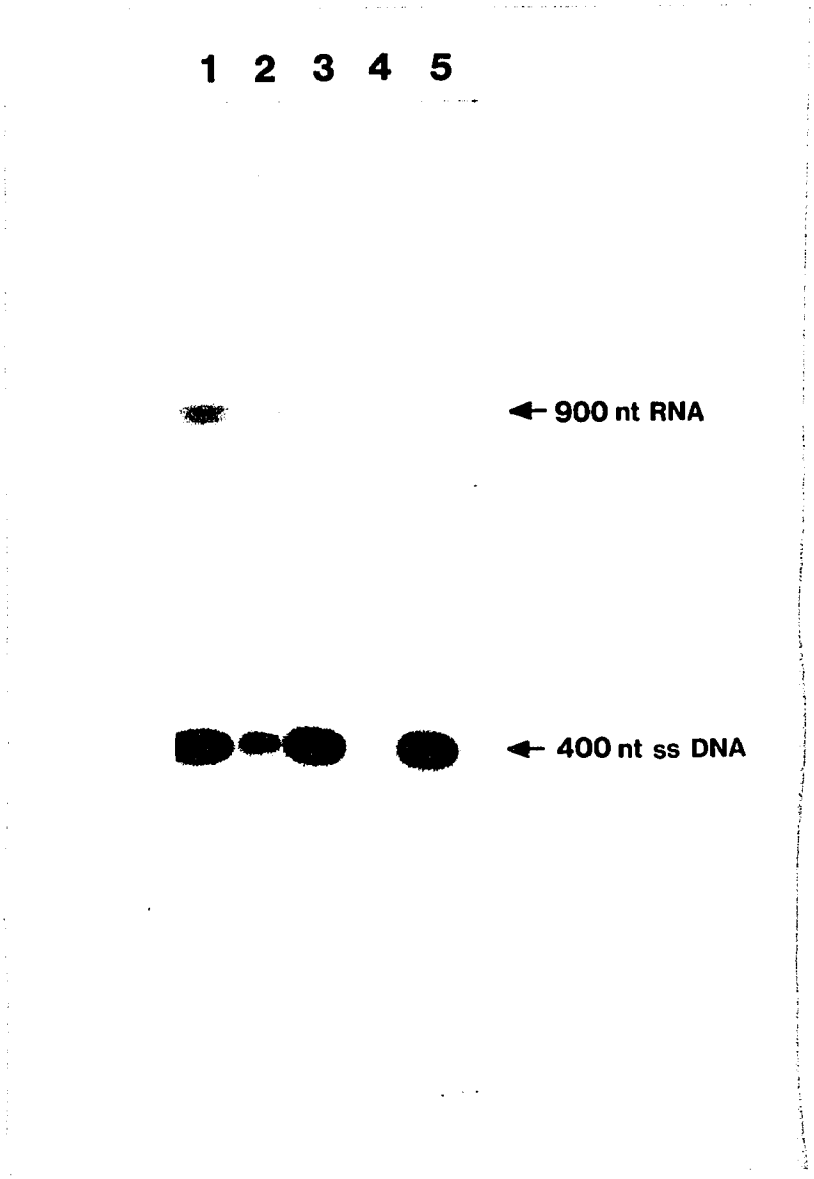
1 2 3 4 5
900 nt RNA
400 nt ss DNA

the S-100 extract was used for further study of ribonuclease activity. The DNase activity of the S-100 extract was inhibited by 10 mM EDTA, while the RNase activity was not inhibited by 10 mM EDTA (lanes 3 and 5 in Fig. 11).

3-9 Construction of an RNA-DNA joint molecule and a single-stranded DNA

As mentioned in Chapter 1, it is now thought that the breakdown of mRNA to the mononucleotide level in *E. coli* is dependent on two 3'-to-5' exoribonucleases, polynucleotide phosphorylase and RNase II. During experiments designed to achieve the biochemical identification of a 5'-to-3' exoribonuclease, we have assumed that a 3'-to-5' exoribonuclease was present in *B. subtilis* extracts. One way to assay the 5'-to-3' exoribonuclease activity in *B. subtilis* extracts is to use differentially labeled RNA as substrate. I attempted to construct an RNA molecule in which the first 9 nucleotides were ^{32}P-labeled and the rest of the molecule was ^{3}H-labeled. Incubation of such a differentially labeled RNA substrate with fraction of cell extracts would release the acid-soluble radioactive labels. If the fraction of cell extracts has the ribonucleolytic activity that degrades this differentially labeled RNA in a 5'-to-3' direction, then we would be able to detect a faster rate of releasing the acid-soluble ^{32}P-label than ^{3}H-label at short time intervals. On the other hand, if the fraction of the cell extracts has the ribonucleolytic activity that degrades this differentially labeled RNA in a 3'-to-5' direction, then a faster rate of releasing the acid-soluble ^{3}H-label than ^{32}P-label would be observed. However, it was

very difficult to construct such a differentially labeled RNA by in vitro transcription using T7 RNA polymerase (see Appendix B in Chapter 5). Another strategy to assay a 5'-to-3' exoribonuclease activity in the presence of 3'-to-5' exoribonuclease activity was to use an RNA-DNA joint molecule as substrate. Under the conditions that inhibit the nucleolytic decay of DNA (Fig. 11), the RNA moiety of an RNA-DNA joint molecule could be degraded by either a 5'-to-3' exoribonuclease or an endoribonuclease, but not by a 3'-to-5' exoribonuclease.

To construct a linear RNA-DNA joint molecule (see Fig. 12), an unlabeled 101-nt RNA primer was prepared by in vitro transcription of *Sal*I-linearized pYH3 and annealed to the EE60 ssDNA, which contains the *ermC* template strand. The 3' end of the 101-nt RNA was then used as a primer for extension by Sequenase Version 2.0 in the presence of [α-^{32}P]dATP. Digestion of the extended product with *Hpa*I yielded a 700-nt RNA-DNA "joint molecule" which was ^{32}P-labeled in its DNA moiety. This 700-nt RNA-DNA joint molecule was degraded to a 600-nt ssDNA by DNase-free pancreatic RNase (Fig. 13A), indicating that RNA was indeed present in the 5' moiety of the joint molecule.

As a control for nucleolytic decay of DNA, a ssDNA molecule was constructed based on the method similar to that of the RNA-DNA joint molecule. An M13 "-40" sequencing primer was annealed an M13mp19 derivative that contained a 360-nt insert representing *Sac*I-*Bcl*I fragment of *ermC*. Primer extension products were labeled with [α-^{32}P]dATP and digested with *Hin*dIII. The 400-nt ^{32}P-labeled ssDNA was isolated from a denaturing polyacrylamide gel.

Figure 12. Construction of RNA-DNA joint molecules.

Transcription of *Sal*I-linearized pYH3 by T7 RNA polymerase produced an 101-nt RNA runoff transcript, indicated by thick bar. Thin lines represent single-stranded DNA. The isolated 101-nt RNA primer was annealed to EE60 ssDNA, which contained the *ermC* template strand. The primer was extended by Sequenase Version 2.0 in the presence of [α-^{32}P]dATP, followed by digestion with *Hpa*I. The reaction mixture was run on a 1.0% agarose-6.6M formaldehyde gel and RNA-DNA joint molecules were isolated from the gel.

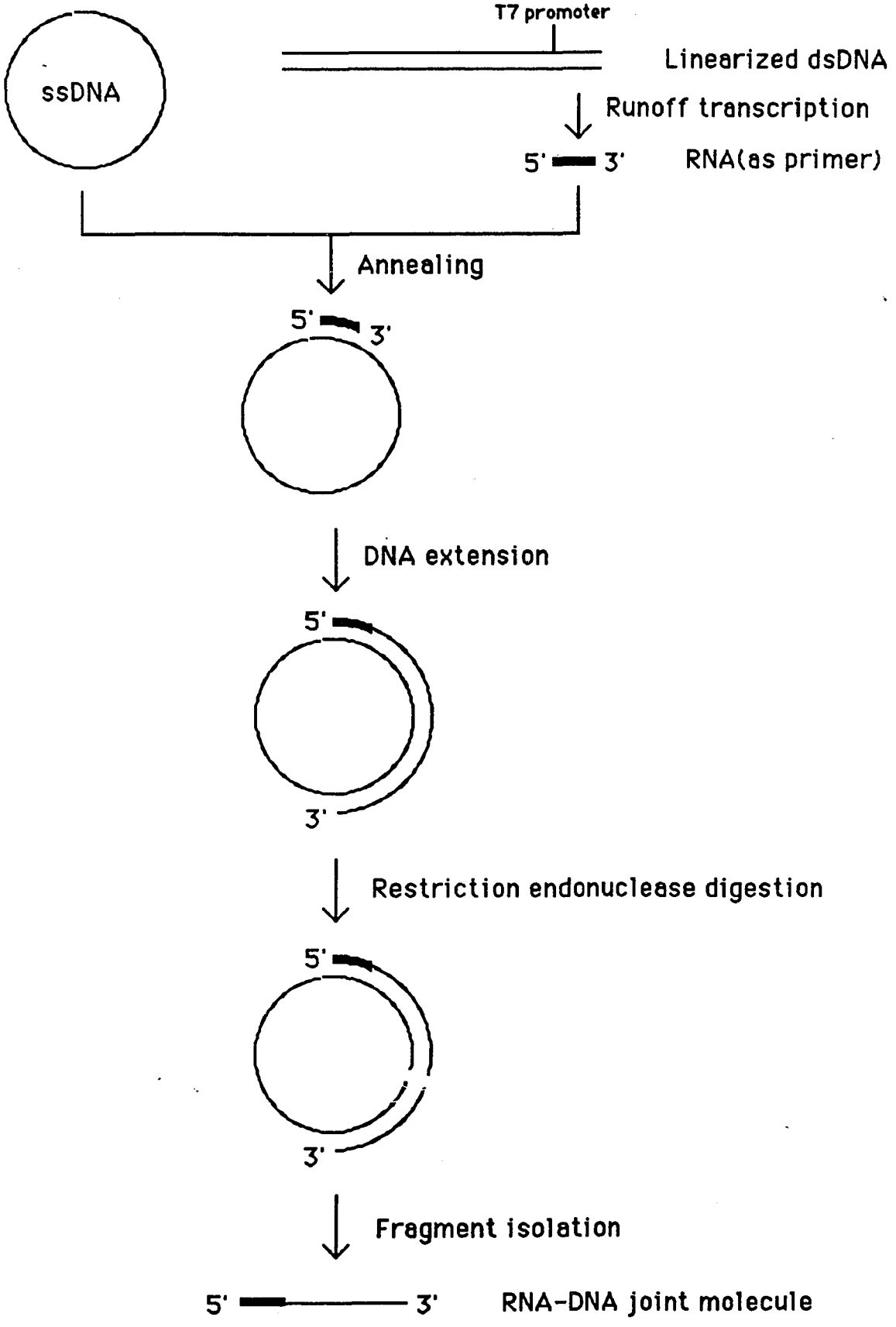
T7 promoter
ssDNA
Linearized dsDNA
Runoff transcription
5'
3'
RNA(as primer)
Annealing
5'
3'
DNA extension
5'
3'
Restriction endonuclease digestion
5'
3'
Fragment isolation
5'
3'
RNA-DNA joint molecule

3-10 Decay of an RNA-DNA joint molecule in the *B. subtilis* extract

The ^{32}P-labeled 700-nt RNA-DNA joint molecule and 400-nt ssDNA were incubated with an S-100 extract at 25°C in the presence or absence of EDTA. A time course of incubation is shown in Fig. 13B. In the presence of EDTA, the degradation of the 400-nt ssDNA was inhibited, but the 700-nt RNA-DNA joint molecule was gradually degraded to give a broad band of around 600-nt size (lanes 1 to 5 in Fig. 13B). The 600-nt product of digestion is similar in size to the ssDNA product produced from DNase-free pancreatic RNase digestion of the 700-nt RNA-DNA joint molecule (Fig. 13A). In the absence of EDTA, both the RNA-DNA joint molecule and ssDNA were degraded during the incubation, as expected (lanes 6 to 10 in Fig. 13B).

When the 700-nt RNA-DNA joint molecule was digested with DNase-free pancreatic RNase, a single 600-nt ssDNA product was seen (Fig. 13A). Pancreatic RNase is a heterogeneous mixture of ribonucleases isolated from bovine pancreas, and the RNA moiety is degraded completely by these RNases. However, it is not clear why a broad band of degradation products was observed when the 700-nt RNA-DNA joint molecule was incubated with the S-100 extract. It is possible that the S-100 extract contains endoribonucleases that produce multiple cleavages at the RNA moeity of the joint molecule. Another possible explanation is that a 5'-to-3' exoribonuclease in the extract degrades RNA moiety of the joint molecule from 5' end and slows down at RNase pause site. Mapping 5' ends of these decay intermediates is necessary to see whether the 5' ends of these RNA moieties correspond to regions of the predicted secondary structure.

Figure 13. Decay of an RNA-DNA joint molecule.

(A) Conversion of a linear RNA-DNA joint molecule to a ssDNA molecule by DNase-free pancreatic RNase. The 700-nt RNA-DNA molecule in which the DNA moiety was ^{32}P-labeled, and the 400-nt ^{32}P-labeled ssDNA molecule were incubated at 37°C with DNase-free pancreatic RNase. The digestion products were extracted with phenol at 0 and 20 min (lanes 1 and 2, respectively). The same substrate mix was incubated with a *B. subtilis* extract S-100. The reaction mixtures were extracted with phenol at 0 and 20 min (lane 3 and 4, respectively). Samples were analyzed on a 6% polyacrylamide gel and visualized by autoradiography. (B) Time course of digestion of the RNA-DNA joint molecule by an S-100 extract. The ^{32}P-labeled RNA-DNA joint molecule and ssDNA were incubated in the presence (+) and absence (-) of EDTA at 25°C with an S-100 extract. The incubation time (in minutes) is indicated above each lane. Aliquots containing 30 µl of the digest were extracted with phenol and analyzed electrophoretically (see Section 2-10).

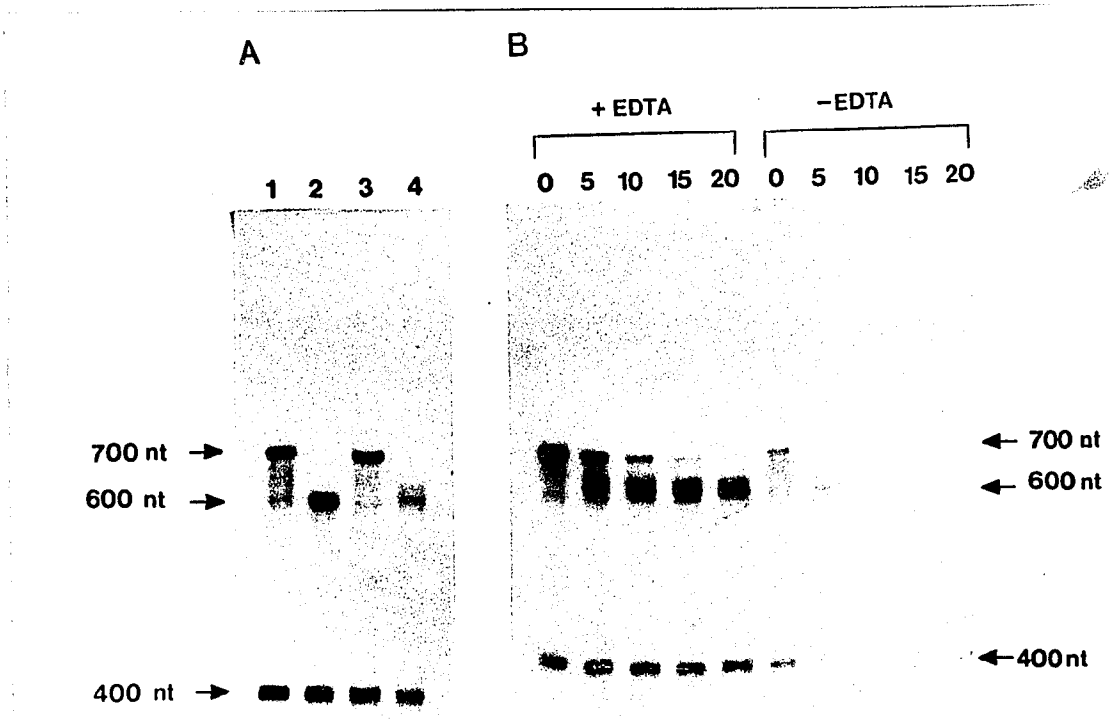
A
B
+ EDTA
−EDTA
1 2 3 4
0 5 10 15 20 0 5 10 15 20
700 nt
600 nt
400 nt
700 nt
600 nt
400nt

The degradation of the 700-nt RNA-DNA joint molecule to the 600-nt ssDNA under conditions in which ssDNA decay is inhibited shows that the RNA moiety at the 5' segment of the joint molecule is degraded either by a 5'-to-3' exoribonuclease, or by an endoribonuclease followed by 3'-to-5' exoribonucleolytic decay of the upstream RNA, or by multiple endoribonucleases. The experiment described in the next section was designed to further assess the relative likelihoods of these two possibilities.

3-11 Decay analysis of a circular RNA in vitro

To test whether the 101-nt RNA moiety of the RNA-DNA joint molecule was degraded endonucleolytically, attempts were made to circularize a uniformly labeled 101-nt RNA by T4 RNA ligase. The idea was to test whether the circular RNA could be degraded by the *B. subtilis* extract. However, it seems to be very difficult to ligate the 5'-phosphoryl terminal of this 101-nt RNA with its 3'-hydroxyl end, probably because its secondary structure prevents the ends from contacting each other.

Since it is easier to self-ligate RNA that consists of less than 20 nucleotides by T4 RNA ligase (O. Uhlenbeck, personal communication), we decided to construct a circular RNA that consisted only of the 5'-proximal 18 nucleotides from the 700-nt RNA-DNA joint molecule. Plasmid pYH4, a derivative of pYH3, has a *Kpn*I site which was introduced by oligonucleotide-directed mutagenesis (Fig. 9). Transcription of *Kpn*I-linearized pYH4 yields an 18-nt RNA. T4 RNA ligase can circularize an RNA molecule in which the 5' end has a monophosphoryl group and the 3' end has a

hydroxyl group. Since GMP can be effectively used for transcription initiation by T7 RNA polymerase, an 18-nt RNA that contained a monophosphoryl group at the 5' end was synthesized by T7 RNA polymerase and was uniformly labeled with [α-32p]UTP in the presence of 5-fold excess of GMP over GTP. This 18-nt RNA was circularized by T4 RNA ligase. To demonstrate that the product of this reaction was indeed circular, the circularized RNA was digested with polynucleotide phosphorylase (a 3'-to-5' exoribonuclease) or DNase-free pancreatic RNase (mixture of endoribonucleases) for 30 min (lanes 5 and 6 in Fig. 14, respectively). The circularized RNA was digested by DNase-free pancreatic RNase but not by polynucleotide phosphorylase, indicating that it was a circular RNA. Control experiments were also done using the 18-nt linear RNA. The linear RNA was digested within 30 min by either polynucleotide phosphorylase or DNase-free pancreatic RNase (lanes 2 and 3 in Fig. 14, respectively), as expected.

Since pYH4 was not digested completely by *Kpn*I, RNA bands on the top of the gel in Fig. 14 could represent RNA transcribed beyond *Kpn*I site. These long transcripts were digested by polynucleotide phosphorylase and DNase-free pancreatic RNase. Since 95% of DNase-free pancreatic RNase is RNase A, which cleaves preferentially pyrimidines at the 3' side, the RNA fragments detected in lanes 3 and 6 in Fig. 14 might contain a stretch of purines derived from the cleavage of the RNA transcripts. RNA decay intermediates were detected from the digestion of the long transcripts by polynucleotide phosphorylase (see lanes 2 and 5 in Fig. 14).

Figure 14. Decay analysis of the circular RNA.

A linear 18-nt RNA that contained a monophosphoryl group at the 5' end was circularized by T4 RNA ligase. The linear RNA was undigested (lane 1), digested for 30 min at 37°C with polynucleotide phosphorylase (lane 2), or digested for 30 min at 37°C with DNase-free pancreatic RNase (lane 3). The circularized RNA was undigested (lane 4), digested for 30 min at 37°C with polynucleotide phosphorylase (lane 5), or digested for 30 min at 37°C with DNase-free pancreatic RNase (lane 6). The linear RNA was incubated with an S-100 extract at 37°C for 0 and 30 min (lane 7 and 8, respectively). The circularized RNA was incubated with an S-100 extract at 37°C for 0 and 30 min (lane 9 and 10, respectively). After the digestion, the reaction mixture (30 µl) was extracted by an equal volume of phenol and 18 µl of aqeuous phase were removed into 9 µl of DNA sequencing dye mix. Aliquots containing 9 µl of digest were denatured and run on a 20% polyacrylamide-8M urea gel and visualized by autoradiography.

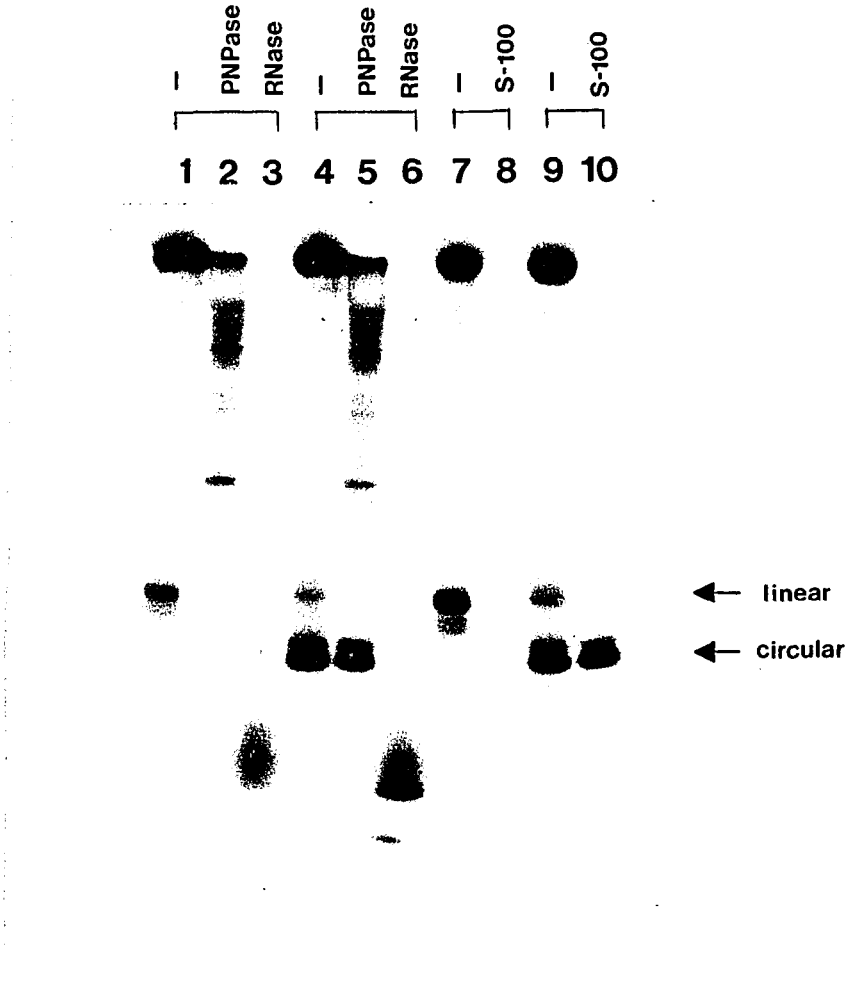
–
PNPase
RNase
–
PNPase
RNase
–
S-100
–
S-100
1 2 3 4 5 6 7 8 9 10
linear
circular

This could be due to the possible secondary structure in RNA transcripts that slows down the progress of polynucleotide phosphorylase from 3' end. The 18-nt circular RNA migrates faster than its linear counterpart in a 20% polyacrylamide-8M urea gel, probably due to its compact structure. The 18-nt circular RNA was incubated at 37°C with an S-100 extract for 0 min and 30 min (lanes 9 and 10 in Fig. 14, respectively). The circular RNA was not degraded while the linear RNA was degraded under the same condition (lanes 7 and 8 in Fig. 14, respectively). These data suggest either that endoribonucleases are not present in *B. subtilis* extract or that if such endoribonucleases are present, the circular 18-nt RNA is not a target for endonucleolytic cleavage.

CHAPTER FOUR

DISCUSSION

4-1 Molecular genetic study on the mechanism of *ermC* mRNA degradation in *B. subtilis*

In order to understand the mechanism of mRNA decay in *B. subtilis*, we studied the induced stability of *ermC* mRNA in this organism. A previous study had shown that the induced stability of *ermC* mRNA requires a ribosome stalled in the leader region while translating the leader peptide coding sequence (Bechhofer and Dubnau, 1987). In this thesis, our working hypothesis to explain the induced stability of *ermC* mRNA was that the 5' end of the message is the target of initiation of decay and a stalled ribosome protects the 5' end against decay. If the 5' end of *ermC* mRNA is the target, then the enzymatic activity responsible for the degradation of the message would be either a 5'-to-3' exoribonuclease or an endoribonuclease which binds to the 5' end of the message and tracks in the 5'-to-3' direction, making endonucleolytic cuts as it progresses.

The results presented in this thesis are consistent with this hypothesis. In RNA molecules with a ribosome stall site positioned internally instead of near the 5' end (pSD100 and pBD362), the sequences upstream of the ribosome stall site were unstable in the presence of Em, while the downstream sequences starting from 57 to 58 nucleotides 5' to SD1 were stable in the presence of Em (Fig. 4 and 5). In an RNA molecule that contained one internal ribosome stall site and another ribosome stall site near the 5' end (pSD132), the full-length RNA was stable in the presence of Em (Fig. 6). The latter result

is not consistent with the explanation that endonucleolytic cleavage of the untranslated upstream sequence was basis for the differential stability of the upstream and downstream RNAs. Therefore, the major decay mode of *ermC* mRNA seems to be 5'-to-3' exonucleolytic degradation rather than endonucleolytic cleavage. In an RNA molecule that contained two internal ribosome stall sites (pSD192), we obtained some evidence that degradation of the full-length RNA was processive in the 5'-to-3' direction (Fig. 7B).

Reverse transcriptase mapping of the uninduced and induced *ermC* mRNAs showed that the 5' end (+1) of the induced *ermC* mRNA is the same as that of the uninduced *ermC* mRNA (Bechhofer and Zen, 1989). Therefore, according to our model for Em-induced stability, the stalled ribosome must be protecting the +1 nucleotide. Although two ribosomes are depicted to stall in the *ermC* leader sequence throughout this thesis (see cartoons in Fig. 2, 4 and 6), it is not clear whether one or two ribosomes stall in the presence of Em. It has been shown that leader peptide codons 3 through 9 are critical for ribosome stalling, based on genetic and biochemical studies (Mayford and Weisblum, 1989; Hue and Bechhofer, 1991). Mayford and Weisblum showed that an Em-bound ribosome stalls with its P and A sites at leader peptide codons 8 and 9. Earlier reports on nuclease protection of mRNA and poly(U) by ribosome binding concluded that 20 nucleotides upstream of the ribosomal P site are covered by the ribosome (Kang and Cantor, 1985; Steitz, 1969; see Gold, 1988 for review). Assuming that an Em-bound ribosome stalls with its P site at codon 8 (which is +43), *ermC* leader sequence between +23 and +43 would be covered by the stalled ribosome. Another ribosome

loading at SD1 (which is +10) might stack behind the Em-bound ribosome and cover the 5' end of *ermC* mRNA. This "two-ribosome stalling" model explains the extremely long half-life of the induced *ermC* mRNA (see below). An alternative model is that only one Em-bound ribosome stalls on the *ermC* transcript. The "one-ribosome stalling" model argues that no ribosomes stack behind because the start codon (which is +22) lies just inside the stalled ribosome and this would prevent another ribosome from loading due to steric hinderance. However, it is difficult to explain how the 5' sequence (+1 to +22) is protected by a single Em-bound ribosome. Perhaps a conformational change of the Em-bound ribosome promotes an interaction between the 5' sequence and stalled ribosome in such a way that the 5' end is protected from ribonucleolytic degradation.

It was surprising at first to find that the 5' ends of the small RNAs were as much as 57 to 58 nucleotides upstream of SD1 (Fig. 5). Assuming that the 5' ends of these RNAs were due to protection by a ribosome stalled at SD1, we expected, according to the "two-ribosome stalling" model, that approximately 20 nucleotides upstream of SD1 would be protected. However, it should be noted that in the earlier studies of mRNA-ribosome interactions endoribonucleases were used to determine the extent of the message protected by ribosome binding. Therefore, the protected mRNA fragments represent only the part of the message that is bound within the ribosome. When 3'-to-5' exoribonucleases were used in the ribosome protection assays, much larger fragments were detected (Castle and Singer, 1969), probably because the mRNA that was external to the ribosome came into contact with other areas of the ribosome. Therefore, it is possible

that mRNA sequences located outside the ribosome may come into contact with other areas of the ribosome. These contacts may impede the progress of a 5'-to-3' exoribonuclease activity, resulting in the relatively stable species detected by reverse transcriptase and S1 nuclease analysis (Fig. 5 and 8).

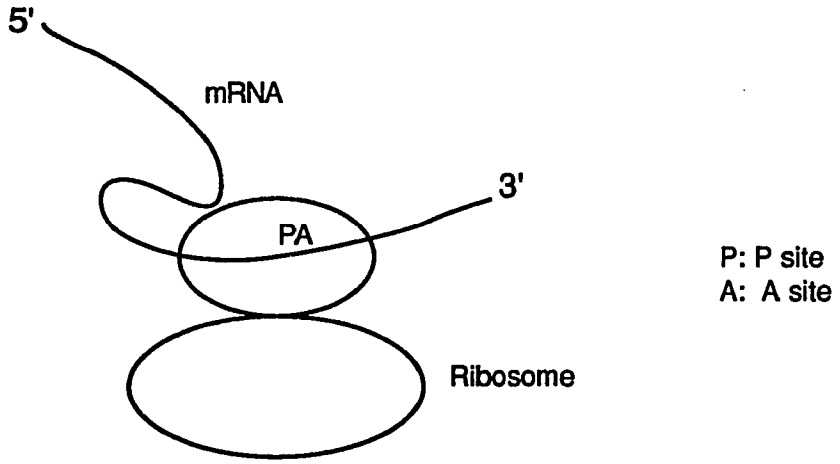

The induced half-lives of the small RNAs encoded by pSD100 and pBD362 (5 to 8 min, see Fig. 4B) is less than the induced half-life of wild-type *ermC* RNA (40 min). This can be explained by our hypothesis. If the 5' end of *ermC* mRNA is the target for decay, then in the wild-type *ermC* mRNA, the backed-up ribosome at SD1 would cover the 5' end, which is only 9 nucleotides upstream of SD1. This coverage would not allow a 5'-end-requiring RNase to initiate degradation of *ermC* RNA, resulting in an extremely long half-life. RNA molecules in which the ribosome stall site was located

internally, however, would have an unprotected 5' end and would be attacked rapidly at the 5' end. Degradation of the sequences downstream of ribosome stall site would be hindered by the stalled ribosome and slowed down, but not stopped at the site of ribosome stalling. Therefore, the small RNAs, which represent downstream RNA sequences protected by ribosome stalling, have a shorter half-life than that of the induced wild-type RNA.

It is also possible that the protection of sequences upstream of SD1 is due to ribosome binding at a site other than SD1. A computer search of the upstream sequences in pSD100 and pBD362 did not reveal any reasonable ribosome binding site followed by open reading frames that could allow a ribosome to bind to the upstream region of SD1. The protection of sequences 57-58 nucleotides upstream of SD1 could also be due to the formation of stable stem-loop structures around the 5' ends of the small RNAs. A computer search for possible stem-loop structures (Devereux et al., 1984), did not predict any strong secondary structure for the region to which the 5' ends of the small RNAs were mapped. The induced stability of an mRNA with 5'-terminal and internal ribosome binding sites encoded by pSD132 is also not due to ribosome loading at the sequences between the 5'-proximal and internal ribosome stall sites since no open reading frames are found in that region.

4-2 Mechanisms of mRNA decay: *B. subtilis* vs. *E. coli*

Despite the recently awakened interest in mRNA degradation in procaryotes, a consensus pathway for mRNA decay has not been established. Polynucleotide phosphorylase and RNase II are 3'-to-5'

exoribonucleases, and RNase III and RNase E are endoribonucleases that have been characterized and shown to play a role in mRNA degradation in *E. coli.* Recently RNase K has been implicated in the endonucleolytic cleavage which initiates the decay of *ompA* and *bla* transcripts (Lundberg at al., 1990). RNase M, an endoribonuclease with rather low specificity has been suggested to be involved in the endonucleolytic decay of *lac* mRNA (Cannistraro and Kennell, 1989). Since no 5'-to-3' exoribonucleases have been identified in *E. coli* (Deutscher, 1985), it is now thought that *E. coli* mRNA is degraded by the combined actions of 3'-to-5' exoribonucleases and endoribonucleases.

The studies in this thesis strongly suggest that *ermC* mRNA is degraded from the 5' end by a 5'-end-requiring RNase, and a ribosome stalled at the 5' leader region provides stability to the whole message. Similar results have been obtained from a study of induced stability of mRNA encoded by *ermA* (another MLS resistance gene) in *B. subtilis* (Sandler and Weisblum, 1989). From the study of *sdh* mRNA degradation in *B. subtilis* (Melin et al., 1990), it has been found that ribosomal loading at the 5' region of this polycistronic mRNA is important for the stability of the whole message. Depriving the first cistron of ribosomes leads to destabilization of the transcript. However, premature termination of translation of the first cistron has little effect on the stability of the *sdh* transcript. These results suggests that the 5' region of *sdh* mRNA is important for controlling stability and initiation of decay, and loading of ribosomes on the 5' region protects the message from the degradation by either an endoribonuclease or a 5'-to-3' exoribonuclease.

Studies on *E. coli ompA* mRNA decay have demonstrated that endonucleolytic cleavage, which occurs 130 nucleotides upstream of ribosome-binding site, initiates decay of this message (Melefors and von Gabain, 1988), and no apparent accumulation of downstream cleavage products have been detected in strains in which the two 3'-to-5' exoribonucleases, polynucleotide phosphorylase and RNase II, have been inactivated (Melefors, 1991). These investigators proposed that the cleavage provides an entry site for a processive decay in the 5'-to-3' direction. Since no 5'-to-3' exoribonucleases have been identified in *E. coli*, these investigators propose that the downstream cleavage products are degraded by an endoribonuclease that tracks from the 5' end and makes endonucleolytic cleavage as it progresses. However, their results could also be interpreted by hypothesizing a 5'-to-3' exoribonuclease. After *ompA* mRNA is cleaved endonucleolytically, a 5'-to-3' exoribonuclease could be activated and could degrade the cleavage products in the 5'-to-3' direction, even in the strains deficient in polynucleotide phosphorylase and RNase II.

Deutscher and Reuven (1991) recently showed that RNase II activity represents close to 90% of the total 3'-to-5' exoribonuclease activity of the *E. coli* extract. Although RNase II-like activity has been characterized from *B. subtilis* extracts isolated from sporulating cells (Kerjan and Szulmajster, 1976), Deutscher and Reuven showed that RNase II-like activity is absent from *B. subtilis* extracts isolated from mid-logarithmic phase cells. The primary mode of RNA degradation in *B. subtilis* extracts was phosphorolytic, implying that a polynucleotide phosphorylase-like activity is present in *B. subtilis* extracts. This enzyme may be involved in mRNA decay in vivo and as

in *E. coli*, we might expect that stem-loop structures at the 3' ends of *B. subtilis* mRNAs will play a role in mRNA stability. In support of this model, it has been reported that the 3' region of the *B. thuringiensis cry* gene enhances the stability of heterologous RNA in both *B. subtilis* and *E. coli* (Wong and Chang, 1986). The *penP* and *cry* gene transcripts terminate beyond the coding sequence with a typical rho-independent terminator sequence in *B. subtilis* . The measured half-lives for *penP* and *cry* mRNAs in *B. subtilis* are 2 min and 6 min, respectively. When the *penP* terminator is replaced by the *cry* terminator, the half-life of the chimeric mRNA is 6 min. Since a stable stem-loop structure can be formed at the 3' end of *cry* mRNA, these investigators proposed that the presence of this structure protects the mRNAs from 3'-to-5' exonucleolytic degradation. However, *penP* mRNA also contains a stem-loop transcription terminator at its 3' end, and it is not known what is different about the *cry* transcription terminator that it can confer stability to upstream sequences.

On the other hand, studies with *ermC* mRNA have shown that the nature of 3' end does not determine mRNA stability. When a 360-bp fragment from the 5' region of *ermC* was fused to the *lacZ* coding sequence (*ermC-lacZ*), several RNAs that contain a 5' *ermC* sequence and different 3' sequences are transcribed that are all inducibly stable (Bechhofer and Dubnau, 1987). This shows that the 5' region of *ermC* mRNA can provide *cis*-dominant stability to diverse 3' ends. Recent studies on three other *ermC* fusion genes showed that transcripts containing a 5' *ermC* sequence and different 3' sequences are also inducibly stable (J. DiMari and D. H. Bechhofer, unpublished

data). Since all of these *ermC* fusion transcripts have rho-independent terminators at their 3' ends, these results may suggest that the stem-loop structure of a transcription terminator at the 3' end of these fusion messages provides a barrier against a 3'-to-5' exoribonuclease. These *ermC* fusion results seem to contradict the results obtained from the *cry* fusion study described above. This contradiction may be resolved by proposing an alternative model to explain the protection of *ermC* mRNA by ribosome stalled at the 5' end. The stalled ribosome may cause a conformational change in mRNA such that ribonucleolytic cleavage sites may not be as accessible to RNases. Based on studies of β-galactosidase expression from *ermA-lacZ* and *ermC-lacZ* fusions (Sandler and Weisblum, 1988; Hue and Bechhofer, 1991), it has been shown that the induced mRNA stability caused by the ribosome stalling does not increase translation of the message. Therefore, it is possible that a conformational change in mRNA caused by the ribosome stalled at the 5' end hinders the accessibility of both RNases and ribosomes.

To demonstrate the importance of a 3'-end stem-loop structure in hindering mRNA decay, a fragment containing a Bs-RNase III target site was cloned into the middle of the *ermC* gene (J. DiMari and D. H. Bechhofer, unpublished data). Bs-RNase III is an endoribonuclease that has been isolated from logarithmically growing *B. subtilis* cells (Panganiban and Whiteley, 1983a). Bs-RNase III shares some characteristics of *E. coli* RNase III and cleaves phage SP82 early mRNAs and rRNA at specific residues in stem-loop structures (Panganiban and Whiteley, 1983b). Recent results from our laboratory show that the transcribed *ermC* mRNA containing a

RNase III target site is unstable in the presence or absence of Em. We propose that there are no endonucleolytic cleavage sites in the wild-type *ermC* mRNA and the instability of the *ermC* mRNA that contains Bs-RNase III cleavage site is due to the endonucleolytic cleavage at the Bs-RNase III target site, followed by rapid decay from the newly formed 3' end by a 3'-to-5' exoribonuclease.

Based on the studies of mRNA decay in *B. subtilis*, a model of mRNA degradation can be proposed. Three different categories of RNases responsible for the decay of mRNA are 5'-to-3' exoribonuclease, endoribonuclease, and 3'-to-5' exoribonuclease. The stem-loop structure located at the 3' end of *B. subtilis* mRNA protects mRNA from degradation by a 3'-to-5' exoribonuclease. If mRNA has an endonucleolytic cleavage site, the decay of mRNA is initiated by endonucleolytic cleavage, followed by exoribonucleolytic decay from 3' end. The 5' end of mRNA is also a target for degradation. However, the ribosomes actively loading in the 5' region of the message or stalled near the 5' end of the transcript could protect mRNA from degradation by a 5'-to-3' exoribonuclease.

4-3 Identification of a 5'-to-3' exoribonuclease activity in *B. subtilis* extracts

Our in vivo studies indicated that the decay of *ermC* mRNA in *B. subtilis* occurs either by a 5'-to-3' exoribonuclease or an endoribonuclease that tracks in the 5'-to-3' direction from the 5' end and makes cuts endonucleolytically. It was then important to identify such an activity in *B. subtilis* extracts. Knowing that a 3'-to-5' exoribonuclease activity is present in *B. subtilis*, the substrates

used for the assay of a 5'-to-3' exoribonuclease activity should be protected from degradation by a 3'-to-5' exoribonuclease. One such substrate is the RNA-DNA joint molecule that contains a DNA moiety at the 3' segment, such that a 3'-to-5' exoribonuclease can not degrade this molecule when DNases are inhibited. When a 700-nt RNA-DNA joint molecule was incubated with the *B. subtilis* S-100 extract under the condition that degradation of DNA was inhibited, the 101-nt RNA moiety of the joint molecule was degraded, yielding a 600-nt ssDNA molecule. This result indicates that the *B. subtilis* extract has either endoribonucleolytic activities or a 5'-to-3' exoribonuclease activity responsible for degrading the 101-nt RNA moiety of the joint molecule. A circular 18-nt RNA containing the 5'-proximal 18 nucleotides of the 700-nt RNA-DNA joint molecule was not degraded by the *B. subtilis* extract, while its linear counterpart was degraded. This result suggests that the *B. subtilis* extract does not contain non-specific endoribonucleolytic activity, although it is possible that this circular 18-nt RNA molecule could have a special conformation that resists endonucleolytic cleavage from the *B. subtilis* extract.

I attempted to construct an RNA-DNA joint molecule that contains this 18-nt RNA at the 5' end, but the yield of the ^{32}P-labeled RNA-DNA joint molecule was so low since the restriction digestion was not efficient. Recently I found that by using the purified 18-nt RNA fragment as the primer, the yield of ^{32}P-labeled RNA-DNA joint molecule was much better. The protocols that I established for synthesis of the joint molecule are now being used for further investigation.

An alternative way to construct an RNA-DNA joint molecule is also being used. Instead of annealing the 18-nt RNA primer to EE61 ssDNA (see Fig. 12), the RNA is being annealed to a synthetic oligonucleotide. The 3' region of this oligonucleotide contains a sequence which is complementary to the 18-nt RNA primer, and the 5' end of these oligonucleotide has oligo(T) sequence. After the 18-nt RNA is annealed to the synthetic oligonucleotide, the RNA primer is extended in the presence of [α-^{32}P]dATP to give a highly labeled RNA-DNA run-off transcript. This run-off approach appears now to be giving a reasonable yield of the RNA-DNA joint molecule (S. Mitra and D. H. Bechhofer, unpublished).

If the RNA moiety of the RNA-DNA joint molecule is degraded by a processive 5'-to-3' exoribonuclease rather than by an endoribonuclease, then the degradation products will predominantly be monoribonucleotides and not oligoribonucleotides. This can be tested by a procedure described recently that was used to characterize a 5'-to-3' exoribonuclease from HeLa cells (Murthy and Manley, 1991). An RNA-DNA joint molecule in which the RNA moiety is ^{32}P-labeled could be synthesized by using ^{32}P-labeled RNA as primer (see Fig. 12). After incubation of the RNA-DNA joint molecule with the *B. subtilis* extract, electrophoresis of the incubation mixture on a 20% polyacrylamide-8 M urea gel should allow detection of the decay products. If the decay products turn out to be predominantly monoribonucleotides that would appear at the bottom of the gel, then the decay should be mediated by a processive 5'-to-3' exoribonuclease. If the decay products turn out to be predominantly oligoribonucleotides, it would imply that the RNA moiety is being

degraded by an endoribonuclease activity. As mentioned before, Bs-RNaseIII is the only characterized endoribonuclease in *B. subtilis* and this enzyme recognizes a stem-loop structure which is not present in our joint molecule. Our RNA-DNA joint molecule could be used to detect the presence of other endoribonucleases in *B. subtilis* extracts.

The presence of a 5'-to-3' exoribonuclease was first implied by showing that reovirus mRNAs with 5' blocking structures such as m7GpppGm or GpppG are resistant to degradation relative to mRNAs with unblocked termini (Furuichi et al., 1977; Shimotohno et al., 1977). It is possible that a 5'-to-3' exoribonuclease in *B. subtilis* can only recognize the uncapped 5' end of mRNA. A capped 18-nt RNA can be synthesized in the presence of a cap analog (Nielson and Shapiro, 1986). A capped RNA-DNA joint molecule can be constructed by using a capped RNA as a primer (see Fig. 12). It would be interesting to know whether the *B. subtilis* extract could degrade the RNA moiety of the capped RNA-DNA joint molecule. Likewise, the 5'-triphosphate end of the RNA-DNA joint molecule could be converted to a 5'-hydroxyl end by alkaline phosphatase. It would also be interesting to know whether the *B. subtilis* extract could degrade the RNA moiety of an RNA-DNA joint molecule with a 5'-hydroxyl end. It is possible that a 5'-to-3' exoribonuclease in *B. subtilis* can only recognize the 5'-triphosphate of mRNA, and mRNAs with 5' blocking structures or 5'-hydroxyl end would be resistant to degradation by this enzyme.

Further fractionation of the *B. subtilis* extract is necessary to isolate and purify a 5'-to-3' exoribonuclease. Dialysis, ammonium sulfate precipitation, and chromatography should be employed to

isolate this enzyme in the near future. Once a 5'-to-3' exoribonuclease has been isolated and characterized, a partial amino acid sequence of this protein can be determined. Based on the amino acid sequences of the peptide from this protein, an oligonucleotide encoding this peptide could be synthesized. Using this specific oligonucleotide as a probe, it will be possible to clone the gene that encodes the 5'-to-3' exoribonuclease. It would be interesting to analyze the decay of mRNA in a *B. subtilis* strain in which the gene for the 5'-to-3' exoribonuclease has been knocked out. These future studies would tell us the role of a 5'-to-3' exoribonuclease in mRNA decay in *B. subtilis*.

CHAPTER FIVE

APPENDIX

A. Plasmids used in this thesis

Plasmid	Relevant Characteristic(s)	Source or Reference
pC194	Plasmid containing chloramphenicol acetyltransferase gene	Horinouchi and Weisblum, 1982b
pE194	Plasmid containing *ermC* gene	Horinouchi and Weisblum, 1982a
pBD142	Plasmid containing *ermC* and chloramphenicol acetyltransferase gene	Fig. 1; Bechhofer and Dubnau, 1987
pBD246	*ermC-lacZ* fusion plasmid	Gryczan et al., 1984
pUB110	Plasmid containing kanamycin resistance gene	Gryczan et al., 1978
pBD9	pE194-pUB110 composite joint at their *XbaI* sites	Hahn et al., 1982
pBD118	pBD9 with the *ermC* promoter deleted	Hahn et al., 1982
pBD362	pBD118 with the pUB110 replication origin deleted	Fig. 8; Bechhofer and Zen, 1989
pBD158	*cop-6* mutant of pBD362	D. Dubnau
pSD1	pBD142 containing 30 base-pair fragment inserted into its unique *Sac*I site	Fig. 3; This thesis
pSD78	pSD1 with original *ermC* -10 sequence inactivated	Fig. 3; This thesis
pSD100	pSD78 containing a tandem insert of a 275-bp *Alu*I sequence from pC194	Fig. 3; This thesis

pSD125	pSD100 derivative with *ermC* -10 sequence deleted	Fig 3; This thesis
pSD132	pSD100 derivative containing two ribosome stall sites, one at the 5' end and one internally	Fig. 3; This thesis
pBD452	pBD142 containing a *Sal*I linker inserted 6 nucleotides downstream of the end of the *ermC* leader peptide sequence	F. Breidt
pSD155	pBD452 derivative containing *Bgl*II and *Hin*dIII sites between -10 and SD1	Fig. 7; This thesis
pSD172	pSD155 derivative containing two ribosome stall sites, one at the 5' end and one internally	Fig. 7; This thesis
pSD192	pSD155 derivative containing two internal ribosome stall sites	Fig. 7; This thesis
pIBI31	T7 polymerase promoter vector	M. Krystal
pYH3	pIBI31 derivative containing 900-base-pair *Hin*dIII-*Cla*I fragment of pSD155 inserted between its *Hin*dIII and *Acc*I sites	Fig. 9; This thesis
pYH4	pYH3 derivative containing *Kpn*I site at +18 position	Fig. 9; This thesis

B. An attempt to construct a differentially labeled RNA molecule

In order to identify a 5'-to-3' exoribonuclease activity in *B. subtilis* extracts, we had to prepare an RNase substrate for assaying this enzymatic activity. Bearing in mind that a 3'-to-5' exoribonuclease was probably present in the cell extract, we wanted to make an RNase substrate that would show a different decay pattern when degraded by a 5'-to-3' exoribonuclease or by a 3'-to-5' exoribonuclease. A differentially labeled RNA molecule in which the 5' portion is labeled by ^{32}P and the 3' portion is labeled by ^{3}H could be used for this purpose. If a fraction of *B. subtilis* extract had only a 3'-to-5' exoribonuclease activity, then incubation of this differentially labeled RNA molecule with that fraction would release a higher percentage of ^{3}H than of ^{32}P in a short incubation time. On the other hand, if a fraction of *B. subtilis* extract had a 5'-to-3' exoribonuclease activity, then incubation of this differentially labeled RNA molecule with that fraction could result in release of a higher percentage of ^{32}P in a short incubation period than the fraction that had no 5'-to-3' exoribonuclease. Since the released nucleotides are acid-soluble, measuring the acid-soluble radioactive count in short time intervals would give us an idea which fraction contained a 5'-to-3' exoribonuclease activity.

To make a differentially labeled RNA substrate, a plasmid pYH3 was constructed (Fig. 9). A 900-bp *Hin*dIII-*Cla*I fragment containing *ermC* sequence was inserted between *Hin*dIII and *Acc*I sites of pIBI31, yielding plasmid pYH3. pYH3 contains a T7 RNA polymerase

promoter followed by the *ermC* leader and coding sequences. Transcription of *Bam*HI-linearized pYH3 gives an *ermC*-sized RNA. The first nine nucleotides transcribed from *Bam*HI-linearized pYH3 by T7 RNA polymerase are pppGGGAGAAGC and the tenth nucleotide is U. In the presence of 12μM [α-^{32}P]GTP, 0.5 mM ATP and 0.5 mM CTP, the 5' 9-nt RNA would be synthesized by T7 RNA polymerase and an enzyme-DNA-RNA ternary complex should be formed since the elongation can not proceed without UTP (Martin et al., 1988). When chased with 0.5 mM [α-^{3}H]UTP and 2.5 mM unlabeled GTP (to compete out the ^{32}P-labeled GTP), the T7 RNA polymerase-linear pYH3 DNA-9-nt RNA ternary complex should continue the transcription, yielding a 900-nt RNA such that the 5' 9-nt RNA is ^{32}P-labeled and the rest of the molecule is predominantly ^{3}H-labeled.

I spent several months working on these pulse and chase experiments. When the *Bam*HI-linearized pYH3 was used as the template, the transcription reaction was done in the presence of 12 μM [α-^{32}P]GTP, 0.5 mM ATP and 0.5 mM CTP. This gave a 9-nt RNA that was ^{32}P-laleled. Chamberlin and coworkers (1987) showed that a stable ternary complex could be formed and isolated by Sephadex G-50 that contains *E. coli* RNA polymerase, the DNA template, and the nascent RNA chain (Levin et al., 1987). Several different columns have been tried to isolate ternary complex. Sephadex G-25 turned out to be the best way to recover the putative ternary complex. The ^{32}P-labeled 9-nt RNA was then chased with the 0.5 mM UTP and unlabeled 2.5 mM GTP. We expected a 900-nt RNA that the 5' end was labeled with ^{32}P. However, we found that the 900-nt RNA was synthesized from the T7 promoter rather than by elongation of the

preformed ^{32}P-labeled 9-nt RNA. This could be due to the dissociation of enzyme-DNA-RNA ternary complex before elongation takes place. This experiment may indicate that T7 RNA polymerase is different from *E. coli* RNA polymerase in that T7 RNA polymerase can not form a stable enzyme-DNA-RNA ternary initiation complex.

CHAPTER SIX

BIBLIOGRAPHY

Arraiano, C. M., S. D. Yancey, and S. R. Kushner. 1988. Stabilization of discrete mRNA breakdown products in *ams pnp rnb* multiple mutants of *Escherichia coli* K-12. *J. Bacteriol.* **170**:4625-4633.

Babitzke P., and S. R. Kushner. 1991. The Ams (altered mRNA stability) protein and ribonuclease E are encoded by the same sructural gene of *Escherichia coli. Proc. Natl. Acad. Sci. USA* **88**:1-5.

Bardwell, J. C. A., P. Regnier, S-M. Chen, Y. Nakamura, M. Grunberg-Manago, and D. L. Court. 1989. Autoregulation of RNase III operon by mRNA processing. *EMBO J.* **8**:3401-3407.

Baga, M., M. Gransson, S. Normark, and B. E. Uhlin. 1988. Processed mRNA with differential stability in the regulation of *E. coli* pilin gene expression. *Cell* **52**:197-206.

Bechhofer, D. H. 1990. Triple post-transcriptional control. *Mol. Microbiol.* **4**(9):1419-1423.

Bechhofer, D. H., and D. Dubnau. 1987. Induced mRNA stability in *Bacillus subtilis. Proc. Natl. Acad. Sci. USA* **84**:498-502.

Bechhofer, D. H., and K. H. Zen. 1989. Mechanism of erythromycin-induced *ermC* mRNA stability in *Bacillus subtilis. J. Bacteriol.* **171**:5803-5811.

Belasco, J. G., J. T. Beatty, C. W. Adam, A. von Gabain, and S. N. Cohen. 1985. Differential expression of photosynthesis genes in *R. capsulata* results from segmental differences in stability within the polycistronic *rxcA* transcript. *Cell* **40**:171-181.

Belasco, J. G., and C. F. Higgins. 1988. Mechanisms of mRNA decay in bacteria: a perspective. *Gene* **72**:15-23.

Berk, A. J., and P. A. Sharp. 1977. Sizing and mapping of early adenovirus mRNAs by gel electrophoresis of S1 endonuclease digested hybrids. *Cell* **12**:721-723.

Brawerman, G. 1987. Determinants of messenger RNA stability. *Cell* **48**:5-6.

Brawerman, G. 1989. mRNA decay: finding the right targets. *Cell* **57**:9-10.

Cannistraro, V. J., M. N. Subbarao, and D. Kennell. 1986. Specific endonucleolytic cleavage sites for decay of *Escherichia coli* mRNA. *J. Mol. Biol.* **192**:257-274.

Castles, J. J., and M. F. Singer. 1969. Degradation of polyuridylic acid by ribonuclease II: protection by ribosomes. *J. Mol. Biol.* **40**:1-17

Chen, C.-Y. A., J. T. Beatty, S. N. Cohen, and J. G. Belasco. 1988. An intercistronic stem-loop structure functions as an mRNA decay terminator necessary but insufficient for *puf* mRNA stability. *Cell* **52**:609-619.

Chen, C.-Y. A., and J. G. Belasco. 1990. Degradation of *pufLMX* mRNA in *Rhodobacter capsulatus* is initiated by nonrandom endonucleolytic cleavage. *J. Bcteriol.* **172**:4578-4585.

Cleveland, D. W., and T. J. Yen. 1989. Multiple determinants of eukaryotic mRNA stability. *The New Biologist* **1**: 121-126.

Contente, S. and D. Dubnau. 1979. Characterization of plasmid transformation in *Bacillus subtilis*: kinetic properties and the effect of DNA conformation. *Mol. Gen. Genet.* **167**:251-258.

Deutscher, M. P. 1985 *E. coli* RNases: making sense of alphabet soup. *Cell* **40**:731-732.

Deutscher, M. P. 1988. The metabolic role of RNases. *TIBS* **13**:136-139.

Deutscher, M. P., and N. B. Reuven. 1991. Enzymatic basis for hydrolytic versus phosphorolytic mRNA degradation in *Escherichia coli* and *Bacillus subtilis*. *Proc. Natl. Acad. Sci. USA* **88**:3277-3280.

Devereux, J., P. Haeberli, and O. Smithies, 1984. A comprehensive set of sequence analysis programs for the VAX. *Nucleic Acids Res.* **12**:387-395.

Donovan, W. P., and S. R. Kushner. 1983. Amplification of ribonuclease II (*rnb*) activity in *Escherichia coli* K-12. *Nucleic Acids Res.* **11**:265-275.

Donovan, W. P., and S. R. Kushner. 1986. Polynucleotide phosphorylase and ribonuclease II are required for cell viability and mRNA turnover in *Escherichia coli* K-12. *Proc. Natl. Acad. Sci. USA* **83**:120-124.

Dubnau, D. 1984. Translational attenuation: the regulation of bacterial resistance to the macrolide-lincosamide-streptogramin B antibiotics. *Crit. Rev. Biochem.* **16**:103-132.

Dubnau, D., and R. Davidoff-Abelson. 1971. Fate of transforming DNA following uptake by competent *Bacillus subtilis*. I. Formation and properties of the donor-recipient complex. *J. Mol. Biol.* **56**:209-221.

Dunn, J. J., and F. W. Studier. 1973. T7 early mRNAs are generated by site-specific cleavage. *Proc. Natl. Acad. Sci. USA* **70**:1559-1563.

Ebbole, D. J., and H. Zalkin. 1988. Detection of *pur* operon-attenuated mRNA and accumulated degradation intermediates in *Bacillus subtilis*. *J. Biol. Chem.* **263**:10894-10902.

Furuichi, Y., A. LaFiandra, and A. J. Shatkin. 1977. 5'-Terminal structure and mRNA stability. *Nature*, **266**:235-239.

Gold, L. 1988. Posttranscriptional regulatory mechanisms in *Escherichia coli*. *Annu. Rev. Biochem.* **57**:199-233.

Graves, M. C., and J. C. Rabinowitz. 1986. In vivo and in vitro transcription of the *Clostridium pasteurianum* ferredoxin gene. *J. Biol. Chem.* **261**:11409-11415.

Gryczan, T. J., S. Contente, and D. Dubnau. 1978. Characterization of *Staphylococcus aureus* plasmids introduced by transformation into *Bacillus subtilis*. *J. Bacteriol.* **134**:318-329.

Gryczan, T. J., G. Grandi, J. Hahn, S. Contente, and Dubnau. 1982. Replication and incompatibility properties of plasmid pE194 in *Bacillus subtilis*. *J. Bacteriol.* **152**:722-735.

Gryczan. T. J., G. Grandi, J. Hahn, R. Grandi, and Dubnau. 1980. Conformational alteration of mRNA structure and the posttranscriptional regulation of erythromycin-induced drug resistance. *Nucleic Acids Res.* **8**:6081-6097.

Gryczan T. J., M. Israeli-Reches and D. Dubnau. 1984. Induction of macrolide-lincosamide-streptogramin B resistance requires ribosome able to bind inducer. *Mol. Gen. Genet.* **194**:357-361.

Guerry, P., D. J. LeBlanc, and S. Falkow. 1973. General method for the isolation of plasmid deoxyribonucleic acid. *J. Bacteriol.* **116**:1064-1066.

Hahn, J., G. Grandi, T. J. Gryczan, and D. Dubnau. 1982. Translational attenuation of *ermC*: a deletion analysis. *Mol. Gen. Genet.* **186**:204-216.

Horinouchi, S., and B. Weisblum. 1982a. Nucleotide sequence and functional map of pE194, a plasmid that specifies inducible resistance to macrolide, lincosamide, and streptogramin type B antibiotics. *J. Bacteriol.* **150**:804-814.

Horinouchi, S., and B. Weisblum. 1982b. Nucleotide sequence and functional map of pC194, a plasmid that specifies chloramphenicol resistance. *J. Bacteriol.* **150**:815-825.

Hu, N., and J. Messing. 1982. The making of strand-specific M13 probes. *Gene* **17**:271-277.

Hue, K. K., and D. H. Bechhofer. 1991. Effect of *ermC* leader region mutations on induced mRNA stability. *J. Bacteriol.* **173**:3732-3740.

Kang, C., and C. R. Cantor. 1985. Structure of ribosome-bound messenger RNA as revealed by enzymatic accessibility studies. *J. Mol. Biol.* **181**:241-251.

Kennell, D. E. 1986. The instability of messenger RNA in bacteria. In W. S. Reznikoff and L. Gold (ed.), "Maximizing Gene Expression", pp. 101-142, Butterworths, Stoneham, Massachusetts.

Kerjan, P., and J. Szulmajster. 1976. Isolation and properties of a cyclic guanosine-monophosphate sensitive intracellular ribonucleas from *Bacillus subtilis*. *Biochimie* **58**:533-541.

King T. C., R. Sirdeskmukh, and D. Schlessinger. 1986. Nucleolytic processing of ribonucleic acid transcripts in procaryotes. *Microbiol. Rev.* **50**:428-451.

Kinscherf, T. G., and D. Apirion. 1975. Polynucleotide phosphorylase can participate in decay of mRNA in *Echerichia coli* in the absence of ribonuclease II. *Mol. Gen. Genet.* **139**:357-362.

Klug, G., and S. N. Cohen. 1990. combined actions of multiple hairpin loop structures and sites of rate-limiting endonucleolytic cleavage determine differential degradation rates of individual segments within polycistronic *puf* operon mRNA. *J. Bacteriol.* **172**:5140-5146.

Klug, G., and S. N. Cohen. 1991. Effects of translation on degradation of mRNA segments transcribed from the polycistronic *puf* operon of *Rhodobacter capsulatus. J. Bacteriol.* **173**:1478-1484.

Kunkel, T. A., J. D. Roberts, and R. A. Zakour. 1987. Rapid and efficient mutagenesis without phenotypic selection. *Methods Enzymol.* **154**: 367-382.

Kuwano, M., M. Ono, H. Endo, K. Hori, K. Nakamura, Y. Hirota, and Y. Ohnishi. 1977. Gene affecting longevity of messenger RNA: a mutant of *Escherichia coli* with altered mRNA stability. *Mol. Gen. Genet.* **154**:279-285.

Lasater, L. S., and D. C. Eichler. 1984. Isolation and properties of a single-strand 5'-to-3' exoribonuclease from Ehrlich ascites tumor cell nucleoli. *Biochemistry* **23**:4367-4373.

Levin J. R., B. Krummel, and M. J. Chamberlin. 1987. Isolation and properties of transcribing ternary complexes of *Escherichia coli* RNA polymerase positioned at a single template base. *J. Mol. Biol.* **196**:85-100.

Lundburg, U., G. Nilsson, and A. von Gablin. 1988. The differential stability of the *Escherichia coli ompA* and *bla* mRNA at various growth rates is not correlated to the efficiency of translation. *Gene* **72**:141-149.

Martin, C. T., D. K. Muller, and J. E. Coleman. 1988. Processivity in early stages of transcription by T7 RNA polymerase. *Biochemistry.* **27**:3966-3974.

Maxam A. M., and W. Gilbert. 1980. Nucleotide sequencing techniques. In L. Grossman and K. Moldave (ed.), "Method in Enzymology", pp. 499-560, Academic Press, New York.

Mayford, M., and B. Weisblum. 1989. *ermC* leader peptide: amino acid sequence critical for induction by translational attenuation. *J. Mol. Biol.* **206**:69-79.

Melefors, O. 1991. The mechanism of *ompA* mRNA degradation in *E. coli.* Ph.D. thesis. Department of Bacteriology, Karolinska Institutet, Stockholm, Sweden.

Melefors, O., and A. von Gabain. 1988. Site-specific endonucleolytic cleavages and the regulation of stability of *E. coli ompA* mRNA. *Cell* **52**:893-901.

Melefors, O., and A. von Gabain. 1991. Genetic studies of cleavage-initiating mRNA decay and processing of ribosomal 9S RNA show that the *Escherichia coli ams* and *rne* loci are the same. *Mol. Microbiol.* **5**(4):857-864.

Melin, L., H. Friden, E. Dehlin, L. Rutberg, and A. von Gabain. 1990. The importance of the 5'-region in regulating the stability of *sdh* mRNA in *Bacillus subtilis. Mol. Microbiol.* **4**(11):1881-1889.

Morikawa, N. and F. Imamoto. 1969. Degradation of tryptophan messenger. *Nature* **223**:37-40.

Morse, D. E., R. Mosteller, R. F. Baker, and C. Yanofsky. 1969. Direction of in vivo degradation of tryptophan messenger RNA- a correction. *Nature* **223**:40-43.

Mott, J. E., J. L. Galloway, and T. Platt. 1985. Maturation of *Escherichia coli* tryptophan operon mRNA: evidence of 3' exoribonucleolytic processing after rho-dependent termination. *EMBO J.* 4:1887-1891.

Mudd. E. A., A. J. Carpousis, and H. M. Krisch. 1990. *Escherichia coli* RNase E has a role in the decay of bacteriophage T4 mRNA. *Genes Dev.* **4**:873-880.

Mudd. E. A., P. Prentki, D. Belin, and H. M. Krisch. 1988. Processing of unstable bacteriophage T4 gene 32 mRNAs into a stable species requires *Escherichia coli* ribonuclease E. *EMBO J.* **7**:3601-3607.

Murthy, K. G. K., P. Park, and J. L. Manley. 1991. A nuclear micrococcal-sensitvie, ATP-dependent exoribonuclease degrades uncapped but not capped RNA substrates. *Nucleic Acid Res.* **19**:2685-2693.

Narayanan, C. S., and D. Dubanu. 1987. Demonstration of erythromycin-dependent stalling of ribosomes on the *ermC* leader transcript. *J. Biol. Chem.* **262**:1766-1771.

Newbury, S. F., N. H. Smith, and C. F. Higgins. 1987. Differential mRNA stability controls relative gene expression within a polycistronic operon. *Cell* **51**:1131-1143.

Nielson D. A., and D. J. Shapiro. 1986. Preparation of capped RNA transcripts using T7 RNA polymerase. *Nucleic Acid Res.* **14**:5936.

Nilsson, G., J. G. Belasco, S. N. Cohen, and A. von Gabain. 1984. Growth-rate dependent regulation of mRNA stability in *Escherichia coli*. *Nature* **312**:75-77.

Nilsson, G., J. G. Belasco, S. N. Cohen, and A. von Gabain. 1987. The effect of premature termination of translation on mRNA stability depends on the location of ribosome release. *Proc. Natl. Acad. Sci USA* **84**:4890-4894.

Ono, M., and M. Kuwano. 1979 A conditional lethal mutation in an *Escherichia coli* strain with a longer lifetime of messenger RNA. *J. Mol. Biol.* **129**:343-357.

Panganiban, A. T., and H. R. Whiteley. 1983a. Purification and properties of a new *Bacillus subtilis* RNA processing enzyme. *J. Biol. Chem.* **258**:12487-12493.

Panganiban, A. T., and H. R. Whiteley. 1983b. *Bacillus subtilis* RNase III cleavage sites in phage SP82 early mRNA. *Cell* **33**:907-913.

Portier, C., L. Dondon, M. Grunberg-Manago, and P. Regnier. 1987. The first step in the functional inactivation of the *Escherichia coli*

polynucleotide phosphorylase messenger is a ribonuclease III processing at the 5' end. *EMBO J.* **6**:2165-2170.

Raleigh, E. A., K. Lech, and R. Brent. 1989. In F. M. Ausubel et al (ed.), "Current Protocols in Molecular Biology", Unit 1.4, Publishing Associates and Wiley Interscience, New York.

Reeve, J. N., and J. B. Cornett. 1975. Bacteriophage SP01-induced macromolecular synthesis in minicells of *Bacillus subtilis. J. Virol.* **15**:1308-1316.

Reeve, J. N., N. H. Mendelson, S. I. Coyne, L. L. Hallock, and R. M. Cole. 1973. Minicells of *Bacillus subtilis. J. Bacteriol.* **114**:860-873.

Regnier P., and M Grunberg-Manago. 1989. Cleavage by RNase III in the transcripts of the *metY-nusA-infB* operon of *Escherichia coli* releases the tRNA and initiates the decay of the downstream mRNA. *J. Mol. Biol.* **210**:293-302.

Regnier P., and E. Hajnsdorf. 1991. Decay of mRNA encoding ribosomal protein S15 of *Escherichia coli* is initiated by an RNase E-dependent endoribonucleolytic cleavage that removes the 3' stabilizing stem and loop structure. *J. Mol. Biol.* **217**:283-292.

Saini, K. S., I. C. Summerhayes, and P. Thomas. 1990. Molecular events regulating messenger RNA stability in eukaryotes. *Mol. Cell. Biochem.* **96**:15-23.

Sandler, P., and B. Weisblum. 1988. Erythomycin-induced stabilization of *ermA* messenger RNA in *Staphylococcus aureus* and *Bacillus subtilis. J. Mol. Biol.* **203**:905-915.

Sandler, P., and B. Weisblum. 1989. Erythromycin-induced ribosome stall in the *ermA* leader: a barricade to 5'-to-3' nucleolytic cleavage of the *ermA* transcript. *J. Bcteriol.* **171**:6680-6688.

Schmeissner, U., K. McKenney, M Rosenberg, and D. Court. 1984. Removal of a terminator structure by RNA processing regulates *int* gene expression. *J. Mol. Biol.* **176**:39-53.

Shimotohno, K., Y. Kamada, J. Hashimoto, and K. Miura. 1977. Importance of 5-terminal blocking structure to stabilize mRNA in eukaryotic protein synthesis. *Proc. Nat. Acad. Sci. USA* **74**:2734-2738.

Shivakumar, A. G., and D. Dubnau. 1981. Characterization of a plasmid-specified ribosome methylase associated with macrolide resistance. *Nucleic Acids Res.* **9**:2549-2564.

Shivakumar, A. G., J. Hahn, and D. Dubanu. 1979. Studies on the synthesis of plasmid-coded proteins and their control in *Bacillus subtilis* minicells. *Plasmid* **2**:279-289.

Shivakumar, A. G., J. Hahn, G. Grandi, Y. Kozlov, and D. Dubnau. 1980. Posttranscriptional regulation of an erythromycin resistance protein specified by plasmid pE194. *Proc. Natl. Acad. Sci. USA* **77**:3903-3907.

Steitz, J. A. 1969. Polypeptide chain intiation: nucleotide sequences of the three ribosomal binding sites in bacteriophage R17 RNA. *Nature* (London) **224**:957-964.

Stevens, A., and M. K. Maupin. 1987. A 5'-to-3' exoribonuclease of human placental nuclei: purification and substrate specificity. *Nucleic Acids Res.* **15**:695-708.

Subbarao, M. N., and D. Kennell. 1988. Evidence for endonucleolytic cleavages in decay of *lacZ* and *lacI* mRNAs. *J. Bacteriol.* **170**:2860-2865.

Taraseviciene, L., A. Miczak, and D. Apirion. 1991. The gene specifying RNase E (*rne*) and a gene affecting mRNA stability (*ams*) are the same gene. *Mol. Microbiol.* **5**(4):851-855.

Ulmanen, I., K. Lundstrom, P. Lehtovaara, M. Sarvas, M. Ruohonen, and I. Palva. 1985. Transcription and translation of foreign genes in *Bacillus subtilis* by the aid of a secretion vector. *J. Bacteriol.* **162**:176-182.

Weisblum, B. 1983. Inducible resistance to macrolides, lincosamides and streptogramin type B antibiotics: the resistance phenotype, its biological diversity, and structural elements that regulate expression. In J. Beckwith, J. Davis, and J. A. Gallant (ed.), "Gene Function in Prokaryotes", pp. 91-121, Cold Spring Harbor Laboratory, Cold Spring Harbor, New York.

Weisblum, B., C. Siddhikol, C. J. Lai, and V. Demohn. 1971. Erythromycin-inducible resistance in *Staphylococcus aureus*: requirements for induction. *J. Bacteriol.* **106**:835-847.

Wong, H. C., and S. Chang. 1986. Identification of a positive retroregulator that stabilizes mRNAs in bacteria. *Proc. Natl. Acad. Sci. USA* **83**:3233-3237.

Yanish-Perron, C., J. Viera, And J. Messing. 1985. Improved M13 phage cloning vectors and host strains: nucleotide sequences of the M13mp18 and pUC19 vectors. *Gene* **33**:103-119.